Deep Sea Research Part I: Oceanographic Research Papers
September 2010, Volume 57, Issue 9, P. 1120-1136
http://dx.doi.org/10.1016/j.dsr.2010.05.011

First insights into the structure and environmental setting of cold-seep communities in the Marmara Sea

Bénédicte Ritt[a, *], Jozée Sarrazin[a, *], Jean-Claude Caprais[a], Philippe Noël[a], Olivier Gauthier[a, b], Catherine Pierre[c], Pierre Henry[d] and Daniel Desbruyères[a]

[a] Ifremer—Centre de Brest, DEEP/LEP, BP 70, 29280 Plouzané, France
[b] Université de Bretagne Occidentale, IUEM, LEMAR (UMR 6539), Technopôle Brest-Iroise, Place Nicolas Copernic, 29280 Plouzané, France
[c] Université Paris 06, LOCEAN (UMR 7159), F-75252 Paris 05, France
[d] CEREGE, Chaire de géodynamique du Collège de France, Europôle de l'Arbois, BP 80, 13545 Aix-en-Provence Cedex 04, France

*: Corresponding author : B. Ritt, J. Sarrazin : benedicte.ritt@ifremer.fr ; jozee.sarrazin@ifremer.fr

Abstract:

A brackish-water cold seep on the North Anatolian Fault (NAF) in the Marmara Sea was investigated with the Nautile submersible during the MarNaut cruise in 2007. This active zone has already been surveyed and revealed evidence of active seeping on the seafloor, such as bubble emissions, patches of reduced sediments, microbial mats and authigenic carbonate crusts. MarNaut was the first opportunity to sample benthic communities in the three most common microhabitats (bioturbated and reduced sediments, carbonate crust) and to examine their relationships with environmental conditions. To do so, faunal communities were sampled and chemical measurements were taken close to the organisms. According to diversity indices, the bioturbated microhabitat exhibited the highest taxonomic diversity and evenness despite a lower number of samples. Conversely, the reduced sediment microhabitat exhibited the lowest taxonomic diversity and evenness. The carbonate crust microhabitat was intermediate although it had the highest biomass. Multivariate analyses showed that (1) fauna were relatively similar within a single microhabitat; (2) faunal community structure varied greatly between the different microhabitats; (3) there was a link between faunal distribution and the type of substratum; and (4) chemical gradients (i.e. methane, oxygen and probably sulphides) may influence faunal distribution. The estimated fluid flow velocity (0.4–0.8 m/yr) confirmed the presence of fluid emission and provided evidence of seawater convection in the two soft-sediment microhabitats. Our results suggest that the reduced sediments may represent a harsher environment with high upward fluid flow, which restrains seawater from penetrating the sediments and inhibits sulphide production, whereas bioturbated sediments can be viewed as a bio-irrigated system with sulphide production occurring at greater depths. Therefore, the environmental conditions in reduced sediments appear to prevent the colonization of symbiont-bearing fauna, such as vesicomyid bivalves, which are more often found in bioturbated sediments. Fluid flow appears to control sulphide availability, which in turn influences the horizontal and vertical distribution patterns of fauna at small spatial scales as observed at other seep sites

Keywords: Marmara Sea; Cold seep; Benthic fauna; Biological diversity; Environmental conditions; Chemosynthetic.

Cold-seep ecosystems are home to chemosynthetic communities composed of a number of endemic vesicomyid, solemyid and mytilid bivalves, as well as several siboglinid polychaetes that are often the dominant macro- and megafauna (Bergquist et al. 2003, 2005; Levin and Mendoza 2007; Levin et al. 2003; Luth et al. 1999; Olu et al. 1996, 1997; Olu-Le Roy et al. 2004, 2007; Paull et al. 1984; Sahling et al. 2002; Sibuet and Olu, 1998). One of the key adaptations of species to seep habitats is their association with bacterial endosymbionts, which ensure chemosynthetic primary production through the oxidation of the reduced compounds contained in the seeping fluids (Cavanaugh, 1983; Childress et al., 1986; Dubilier et al., 2008; Fisher, 1990). Thus, these taxa rely on seeping fluids for their nutrition and survival, and their spatial distribution is a reliable indicator of the presence of chemical fluxes at the sediment-water interface (Levin, 2005; Sibuet and Olu, 1998). Other heterotrophic species live in association with seep chemosynthetic species, benefiting from these enriched environments (Tunnicliffe et al., 2003) and also relying on organic inputs derived from neritic (coastal) and terrestrial organic material (Gage, 2003).

Recent studies on seep ecosystems have highlighted the vast heterogeneity of habitats and associated faunal assemblages at small spatial scales that range from the sampling unit (dm scale) to the geological structure (km scale) on which the assemblages are found (Vanreusel et al., 2009). Although there are some similarities between structures and regions, each newly discovered seep area may have its own signature in terms of faunal structure, diversity and chemical conditions. Previous studies have suggested that the composition and intensity of fluid seepage are the major factors structuring the distribution of seep fauna (Levin, 2005; Sibuet and Olu, 1998). Other driving forces, such as depth (Sibuet and Olu, 1998), substratum type (Olu et al., 1996; Sahling et al., 2003), oxygen concentration (Bergquist et al., 2005; Levin and Gage, 1998), biological interactions (Bergquist et al., 2003) and hydrographic regime (Luth and Luth, 1998; Luth et al., 1999) have also been suggested to play a role on species distribution patterns.

Recently, the deep-sea sites of the Marmara Sea (40-41°N; 26-30°W) have received more attention from the scientific community, mainly because of the seismic hazard in the Istanbul area. This intra-continental sea, located on the North-Anatolian Fault

zone (NAF), is tectonically active (Armijo et al., 2004; Le Pichon et al., 2001; Sengor et al., 2005). Submarine earthquakes constitute a potential threat for human populations (Ambraseys, 2000; Ambraseys and Finkel, 1991; Ansal et al., 2009; Hubert-Ferrari et al., 2000; Oglesby et al., 2008). These earthquakes influence gas emissions (Hovland et al., 2002) as confirmed by the presence of gas flares in the Izmit Gulf following the 1999 Kocaeli earthquake (Alpar, 1999). Subsequent investigations have revealed cold seeps in the deep basins of the Marmara Sea along the main fault, on secondary fault branches and on the anticline ridges (Armijo et al., 2005; Geli et al., 2008; Halbach et al., 2004; Zitter et al., 2008). The most common evidence for fluid expulsion in the Marmara Sea is the presence of black patches of reduced sediments associated with microbial mats and authigenic carbonate crusts (Zitter et al., 2008). While these generally correspond to zones of diffuse flow, focused flow of brackish water has been observed at two sites (Zitter et al., 2008). Moreover, cold seeps can release hydrocarbons as a separate gas phase, and even as oil (Bourry et al., 2009; Geli et al., 2008). Seeps can be thus characterised by gas flares, brackish-water springs or diffuse emission, depending on the dominant mode of fluid emission.

In 2007, the MarNaut cruise represented the first opportunity to sample the fauna associated with the cold-seep ecosystems of the Marmara Sea and to characterise the abiotic conditions of this basin of the eastern Mediterranean Sea. The present study aims to describe the structure of the benthic communities in the three most common microhabitats of a brackish-water cold seep and relate community structure to local environmental factors. Even though these objectives were hindered by sampling limitations, this study represents a fundamental step in advancing our understanding of the ecology and biogeography of chemosynthetic seep species within the larger Mediterranean context.

2. Materials and methods

2.1. Study area

Located between 40-41°N and 26-30°W, the Marmara Sea is the easternmost semi-enclosed basin of the Mediterranean Sea, and connects the Black Sea to the Aegean Sea via the Bosphorus and Dardanelles Straits. It is subdivided into four major basins

from east to west: the Çinarcik, Kumburgaz, Central and Tekirdağ basins, with a maximum depth of about 1260 m in the Central basin (Figure 1).

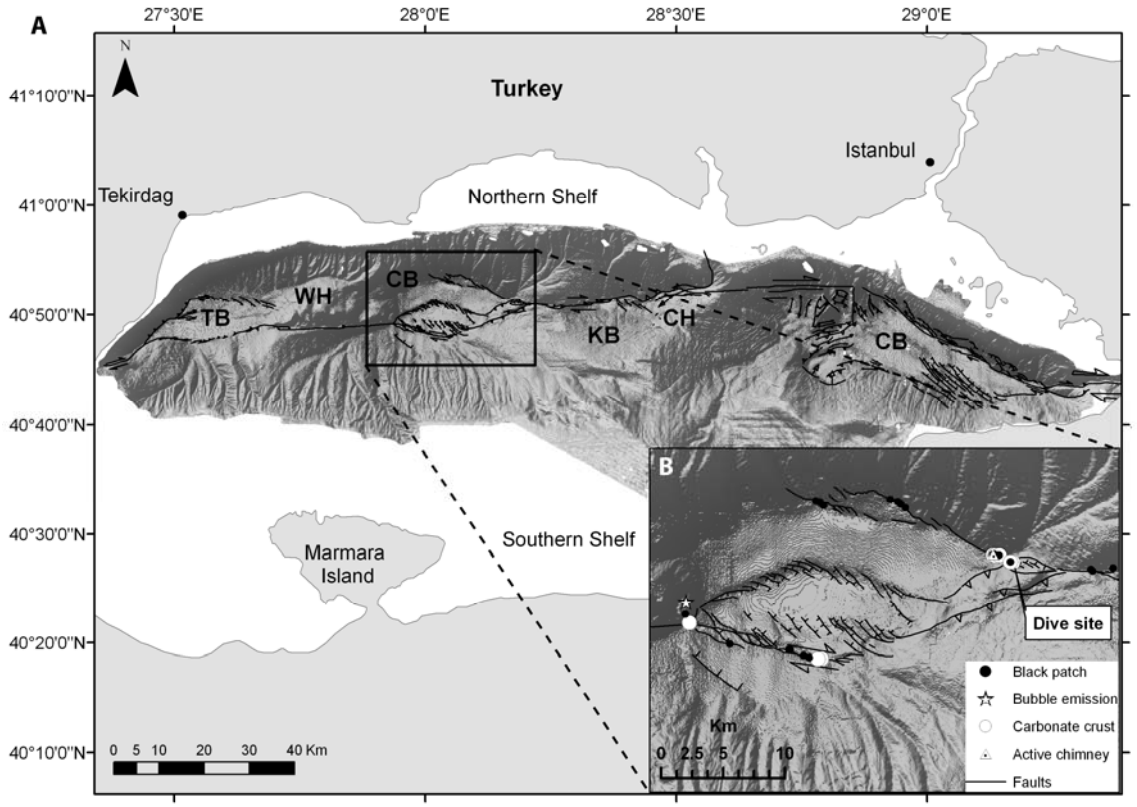

Fig. 1. (A) General bathymetric map of the Marmara Sea showing the fault traces (from Le Pichon et al., 2001), the different geological basins and (B) details of the study area in the Central Basin. The presence of black patches on the seafloor (black dots), carbonate crusts (white dots), active chimney (white triangle) and bubble emission (white star) were mapped according to the observations reported during the MARMARASCARPS cruise (Zitter et al., 2008) and exploratory MarNaut dives. The dive site corresponds to the site dedicated to environmental and faunal sampling during the MarNaut cruise in 2007. Abbreviations: TB, Tekirdağ Basin; CB, Central Basin; CB, Çinacik Basin; KB, Kumburgaz Basin; WH, Western High; CH, Central High.

Preliminary visual observations of the Marmara Sea seafloor and the associated epibenthic communities were carried out using the ROV *Victor 6000* during the MARMARASCARPS cruise in 2002 (Armijo et al., 2005; Zitter et al., 2008). Our observations and sampling were carried out five years later during the MarNaut cruise (2007) on the R/V *L'Atalante* with the manned submersible *Nautile*. During this cruise, exploratory dives were carried out to map seepage occurrences and faunal distributions at selected sites in the four major basins. Five sampling dives took place at the brackish-water spring described in this study. One of these dives was dedicated to sampling the mega- and macrofauna and characterising the

environmental features in the north-east Central basin (40°51.27'N - 28°10.19'W) at a depth of 1 120 m (Figure 1).

2.2. Sampling site

The chosen seep site harboured a mosaic of microhabitats. Three of these were selected and sampled: (1) the bioturbated sediment microhabitat (Bio) was characterised by brown sediments with small bioturbation holes (Figure 2a); (2) large patches of reduced sediment microhabitat (Red) were covered by short polychaete tubes and were surrounded by Bio patches (Figure 2b); and, (3) sparse carbonate crusts were located a couple of meters from Red patches and collectively constitute the Carbonate Crust microhabitat (CC, Figure 2c).

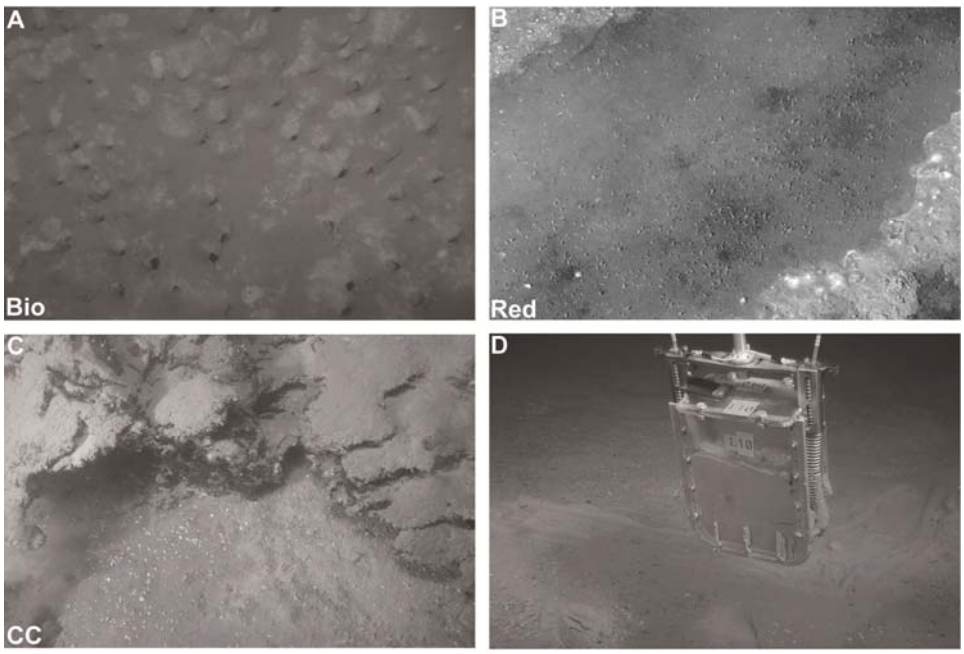

Fig. 2. Photographs of each of the three most common microhabitats of the Marmara cold seeps: (A, Bio) bioturbated sediments, (B, Red) reduced sediments and (C, CC) carbonate crusts (MarNaut cruise, 2007). (D) blade corer used for sampling chemosynthetic communities with the submersible.

Environmental characterisation of each microhabitat was conducted before sampling fauna to avoid any disturbance that could be caused by this sampling. Temperature and salinity measurements were performed using the MicroCat autonomous sensor (F. Harmegnies, Ifremer). Mean values were computed after deploying the sensor for 1 min above the organisms and as close as possible to the seafloor using *Nautile*'s manipulator arm. Water and sediment samples were then taken for chemical analyses using 200 ml titanium bottles and tube corers (30 cm long; 5.4 cm inner

diameter), respectively. Complete sampling details are given in Table 1. Unfortunately, due to time constraints imposed by the use of a manned submersible, the physico-chemical sampling could not be completed above Bio and was not performed above CC. Sediments were also sampled with blade corers (Bayon et al., 2009; Menot et al., 2009, area:0.02m², Figure 2d) deployed by *Nautile*'s arm to collect the epi- and endofauna. The number of samples for each microhabitat varied, depending on time and number of tools available (Table 1).

2.3. Physico-chemical analyses

The 200 ml water samples were used to determine pH as well as methane concentrations. pH measurements were performed on board with a pH-meter connected to a glass electrode (Metreohm) and were corrected for ambient temperature (25°C) and atmospheric pressure. Reproducibility of the method was ±0.01 pH units. Methane concentrations were measured in the laboratory using the headspace technique coupled with a gas chromatograph equipped with a flame-ionisation detector (error of 4%, see details in Sarradin and Caprais, 1996).

Sediments from tube corers were split horizontally on board and pore water was extracted by centrifugation of the different sediment layers (every cm for the first 2 cm and every 2 cm until the end of the core) to measure chlorinity and sulphate concentrations with an ionic chromatograph on an isocratic system DX 120 (DIONEX). Intact cores, along with supernatant water, were used for oxygen measurements. Oxygen profiles within supernatant water and sediments were obtained by using a microsensor OX 100 coupled to a pico-ammeter 5PA 2000 (Unisense) and a micro-manipulator using the Profix data acquisition software (Unisense). The resolution of the sensor was <200 µm. Kendall rank correlations (τ) (Kendall, 1938) were computed between chlorinity and sulphate profiles for the Red and Bio microhabitats.

2.4. Carbonate mineralogy

The mineralogy of the diagenetic carbonates was determined by X ray diffraction. The oxygen and carbon isotopic compositions of carbonates have been measured to characterize the water and carbon sources of the fluids from which the carbonates have precipitated. They are expressed in the conventional δ notation defined as:

$\delta = [(Rs/Rr) - 1] * 1000$, where $R = {}^{18}O/{}^{16}O$ or ${}^{13}C/{}^{12}C$ respectively in the sample (Rs) and in the reference (Rr). The reference for $\delta^{18}O$ and $\delta^{13}C$ is the V-PDB (Craig, 1957; Gonfiantini et al., 1995). The CO_2 gas extracted from the carbonate by attack with 100% phosphoric acid at 90°C was analysed with a triple collector mass spectrometer (ISOPRIME). The analytical precision 2σ is 0.01‰ for both $\delta^{18}O$ and $\delta^{13}C$; the reproducibility is 0.05‰ for $\delta^{18}O$ and $\delta^{13}C$.

2.5. Estimation of fluid velocity in sediments

Since fluid flow velocity influences the distribution of seep faunal assemblages, we have used models of geochemical gradients to estimate fluid flow for the different microhabitats. It is known that the transport of dissolved species such as chloride occurs both through molecular diffusion and advection of interstitial water. The magnitude of diffusive flux and the velocity of advective flow provide constraints for models that can be estimated from the observed chlorinity profiles, a conservative aqueous species. If a steady-state condition is assumed for approximate calculation of the flow velocity, the concentration of dissolved chloride can be described by a partial differential equation (Berner, 1974):

$$D_s\,(d^2C/dx^2)+v(dC/dx)=0$$

where C is the concentration of dissolved chloride (mmol/l), x is the absolute depth (cm) measured downward from the sediment-water interface, D_s is the diffusion coefficient of chloride in sediments (m²/yr), and v is the absolute upward vertical velocity of interstitial water relative to the sediment-water interface (m/yr). The diffusion coefficient used here for this model was 0.036 m²/yr at 14°C for a porosity of 70% and a tortuosity factor of 1.4 (Henry et al., 1996; Li and Gregory, 1974). For all three tube cores, the chlorinity of seawater and of the emissions were assumed to be equal to 583 mmol/l and 496 mmol/l, respectively. Average velocity was fitted to each core. The diffusion coefficient of sulphate in marine sediments is half that of chloride (Iversen and Jørgensen, 1993) and sulphate profiles that would result from the sole effect of diffusion and advection, without any sulphate reduction, were computed assuming a seawater sulphate concentration of 30 mmol/l and an incoming fluid concentration of 0 mmol/l.

2.6. Faunal sorting and identification

Sediments from blade corers dedicated to faunal sampling and sampled at Bio and Red were photographed and split horizontally (0-1, 1-3, 3-5, 5-10, >10 cm) immediately after recovery. Core slices were passed through a sieve column (2 mm, 1 mm, 500 µm, 250 µm) and the retained residues were preserved in 10% buffered formalin. In the laboratory, all sediments were rinsed and invertebrates were sorted under a dissecting microscope and identified to the lowest taxonomic level possible. The CC samples were also washed over a 250 µm mesh and the organisms retained were processed in the same way as those on the soft sediments. Due to space limitations on *Nautile*, two of the crust samples (CC1 and CC2) were put in the same sampling box. While the crusts themselves were treated separately, it was impossible to determine the origin of the material that had fallen to the bottom of the box. This was treated as a combined "sample" (CC_{box}) that was only used when pooling all the carbonate crust data for α-diversity analyses.

The surface of the sampled carbonate crusts was estimated using the IPLab Spectrum® image analysis software. Quantitative 2-D surface analyses were performed on video images, three times for each frame to reduce error resulting from on-screen tracing (Sarrazin and Juniper, 1999). Total surface area was used to calculate area-related indicators, such as density and biomass. However, because it does not take topography into account, this method probably underestimates surface area and in turn overestimates density and biomass.

In this study, we considered macrofauna *sensu stricto* (>250 µm, Hessler and Jumars 1974), so any meiofaunal taxa such as Nematoda, Copepoda and Ostracoda were considered separately. Nevertheless, the resulting meiofaunal list was very incomplete. Meiofauna *sensu stricto* were underestimated since only the fauna retained by a 250 µm mesh was analysed instead of the 32 µm to 62 µm mesh size usually used for this faunal compartment (Hessler and Jumars, 1974; Thistle, 2003; Van Gaever et al., 2006). For most identified taxa, we achieved the family level except for Demospongia, Scyphozoa, Nematoda. While in the first two groups, only one morphology could be distinguished among the specimens, suggesting the presence of a single family, in the latest, several morphologies were identified.

The mean wet weight (ww) was measured for each microhabitat. To do so, individuals of all major macrofaunal taxa (bivalves, polychaetes, gastropods crustaceans) present in a sample were pooled, pat-dried on absorbent paper and weighed on a micro-scale balance with an error of 0.1 mg.

2.7. Faunal diversity analyses

2.7.1. Alpha-diversity

Alpha-diversity analyses were only performed for macrofauna and at the family level, with the exception of Demospongia and Scyphozoa. For meiofauna, only family richness for copepods, ostracods and mites is reported as a measure of alpha-diversity. Rarefaction curves (*sensu* Gotelli and Colwell, 2001) were computed on macrofaunal data for each microhabitat. Rarefaction curves plot expected taxonomic richness against sampling effort (Gauthier et al., 2010*;* Gotelli and Colwell, 2001; Hurlbert, 1971) and helps in evaluating sampling adequacy in different groups of samples. Because of the single sample from Bio, individual-based rarefaction was used in all microhabitats although this assumes homogeneous distribution of individuals and species among samples (Gotelli and Colwell, 2001)

Observed family diversity was also evaluated with commonly used diversity indices as well as more robust intrinsic diversity-based ordering methods. Taxonomic richness (*S*), Shannon's entropy (*H'*, Shannon, 1948) and the Gini-Simpson diversity index (*D*, Gini, 1912; Simpson, 1949) as well as their numbers equivalents were computed. Numbers equivalents express the richness of a hypothetical perfectly even community that is as diverse as the one observed (Jost, 2007; Jost, 2006; Patil and Taillie, 1982). Community evenness was also determined using Pielou's index of evenness (*J'*, Pielou, 1969).

The right tail-sum method (RTS) is a diversity ordering method that allows graphical comparisons of communities (Liu et al., 2007; Patil and Taillie, 1982; Tothmérész, 1998). It was shown to be more robust and stringent than other methods (Liu et al., 2007). Taxonomic groups are ranked by decreasing relative abundance, and the diversity profile is computed as:

303 $$T_i = \sum_{j=i+1}^{S} p_{[j]} \; for \; i = 1, 2, ..., S-1$$

304

305 where T_i is the RTS value at scale i and $p_{[j]}$ is the relative abundance of the j^{th}
306 most abundant taxa. RTS is based on a clear definition of taxonomic diversity and is
307 easily interpretable: communities that systematically have higher T_i values are more
308 diverse. However, if the profile for two communities cross, no conclusion can be
309 drawn (Liu et al., 2007).

310

311 2.7.2. Beta-diversity

312 Despite the modest number of samples, multivariate analyses were conducted to
313 better illustrate the similarities and differences among faunal samples. Principal
314 component analysis (PCA) and Ward's hierarchical clustering were used for this
315 purpose. Macrofaunal and meiofaunal data sets were treated separately and
316 ordination results compared with a Procrustean randomization test (Jackson 1995).
317 The lowest available taxonomic level was used. Abundance data were first Hellinger-
318 transformed in order to preserve Hellinger, rather than Euclidian, distances in PCA
319 (Legendre and Gallagher, 2001). The Hellinger distance has been shown to
320 adequately estimate community resemblance (Legendre and Gallagher, 2001). The
321 equilibrium contribution circle was computed to identify taxa having an important
322 impact on the position of samples in the ordination (Legendre and Legendre, 1998).
323 These results were used to formulate hypothesis about the influence of habitat
324 conditions on the variation in taxonomic composition within and between
325 microhabitats.

326

327 Finally, the Jaccard's similarity $\left(S_{jacc}\right)$ coefficient was used to quantify similarity in
328 terms of shared taxa among samples within microhabitats (Jaccard, 1901). This
329 coefficient does not consider the absence of taxa in both samples and has value
330 between 0 and 1. Mean Jaccard similarity in each microhabitat was computed to
331 evaluate within-group variation.

332

333 All analyses were performed in the R environment (R, Development Core Team
334 2009). Rarefaction curves, diversity indices and diversity profiles were computed

both with the Biodiversity R package (Kindt and Coe, 2005) and functions in Gauthier et al. (2010). Multivariate analyses were carried out using the Vegan package (Oksanen et al., 2008).

3. Results

3.1. Physico-chemical characterisation of microhabitats

3.1.1. Sediment appearance

The length of the tube cores varied from 12 to 20 cm depending on the nature of substratum (Table 1). Bio and Red exhibited visible differences in the upper 10 cm of sediment (Table 2). Based on the photographs taken on board, the oxygenated layer of brown sediments into the Bio sediment cores was thick (about 2 cm) and clearly distinct from the black sediment below. On the contrary, only black sediment was visible in the cores from the Red microhabitat (Table 2).

3.1.2. Salinity, temperature and pH at the sediment-water interface

Continuous measurements at the sediment-water interface showed no variation in salinity or temperature, either between the replicates of the Red microhabitat, or between the Red and Bio microhabitats. Overall, mean salinity was 38.8‰ and mean temperature 14.5°C (Table 2). pH in water samples from Red ranged from 7.89 to 7.94 (Table 2) and did not show important variation between replicates.

3.1.3. Oxygen concentrations in pore water and methane concentrations at the sediment-water interface

Oxygen data were only available for Red. Oxygen concentrations at the sediment-water interface varied from 22.8 to 50.9 µmol/l among the three replicates (Table 2). Concentrations were much lower above Red2 where the oxygen depth penetration was the lowest (0.6 cm, Figure 3a). This sample also exhibited by far the highest methane concentration at the sediment-water interface (0.7 µmol/l, Table 2). Oxygen concentration at the sediment-water interface appeared positively correlated to oxygen depth penetration and negatively correlated to methane concentration at the water-sediment interface, but could not be statistically tested due to the small number of samples (n=3, Table 2, Figure 3a).

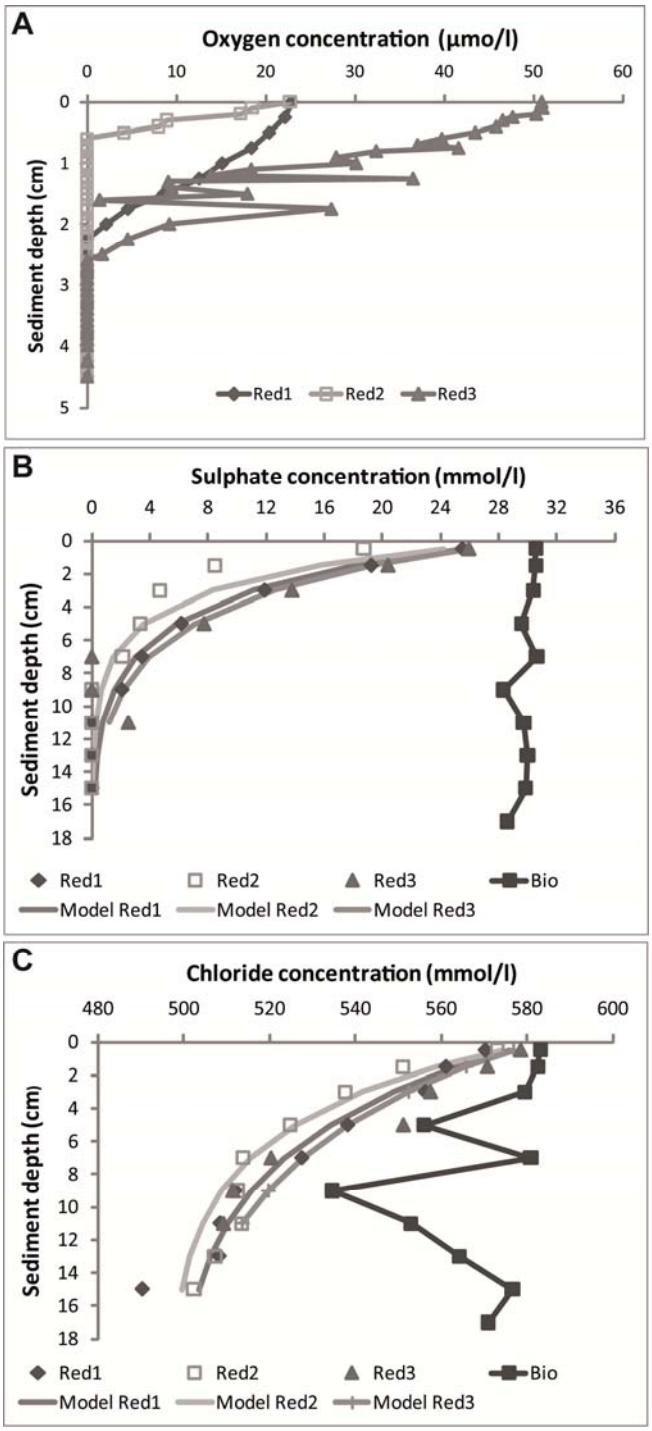

Fig. 3. (A) Dissolved oxygen, (B) sulphate and (C) chloride profiles measured in pore water extracted from sediment cores sampled in the bioturbated sediment (solid line n=1) and reduced sediment (n=3) microhabitats in the Marmara Sea (MarNaut cruise, 2007). The model profiles are represented by dotted lines and explained in the text.

368

369 3.1.4. Isotopic signatures of the carbonate crust

370 The cm-thick carbonate crust sampled is composed of magnesian calcite. Three

371 isotopic measurements were realized on this crust; the upper mm-thick white layer is

underlain by a mm-thick light grey layer that covers a medium grey compact layer. The $\delta^{18}O$ values (+2.40 to +2.09 ‰ V-PDB) are characteristic of calcite precipitated in equilibrium with the Marmara Sea bottom water ; the very low $\delta^{13}C$ values (-35.17 to -45.35 ‰ V-PDB) testify in favour of methane as the major source of carbon, oxidized as CO_2 by methanotrophic bacteria (Aloisi et al., 2000; Gontharet et al., 2007; Pierre and Fouquet, 2007).

3.1.5. Sulphate and chloride concentrations in pore water and estimation of the upward flux velocity

In terms of sulphate and chlorinity, Bio and Red microhabitats exhibited distinctive profiles (Figures 3b, c). The single sulphate profile from Bio was higher than all those from Red. Sulphate concentrations in Bio stayed almost unchanged throughout the different sediment layers, varying from 28.3 to 30.6 mmol/l (Figure 3b). On the other hand, sulphate concentrations in Red decreased sharply in the first 2-3 cm. All dropped to zero at depths of 7 to 11 cm, but Red3 showed a new, slight surge at 11 cm (Figure 3b). The chlorinity profile in Bio presented sharp variations that were apparently independent of depth. Concentrations varied from 535 to 583 mmol/l and, as for sulphate, chloride concentration was higher at Bio than at Red (Figure 3c). Sulphate and chlorinity profiles were positively correlated within each microhabitat (Kendall's τ =0.9, p<0.01 in Bio; τ =0.7, p<0.001 in Red).

The theoretical advection-diffusion profiles of sulphate showed closer fits with actual data for Red1 and Red3. At Red2, the measured sulphate concentrations were lower in the first 4 cm, but match the theoretical advection-diffusion profile at greater depths (Figure 3b). It is not possible to determine whether sulphate reduction occurs in Red.

The shape of the chloride concentration profiles in Red1, Red2 and Red3 reflects upward migration of interstitial water through the sediment layer (Figure 3c). Based on the advection-diffusion model, mean square best fits were obtained for upward velocities (v) of 0.58±0.08 m/yr, 0.75±0.1 m/yr and 0.51±0.07 m/yr for Red1, Red2 and Red3, respectively (Figure 3c). Despite the uncertainty linked to certain factors and the problems inherent to the diffusion of salts, we assumed that the effective diffusivity at our site ranged from 0.03 to 0.04 m^2/yr. Even though the pressure gradient was not measured, it is possible to give a lower bound to permeability in the

406 Red microhabitat from the assumption that the pore pressure gradient probably does
407 not exceed the local lithostatic pressure gradient. Therefore, for a porosity of 70%
408 and hence a density of 1500 kg/m^3, this lower bound ranges from 2 to 4 × 10^{-15} m^2.
409
410 3.2. Macro- and meiofaunal community description
411 3.2.1. Composition, abundance, density and α-diversity
412 Overall, a total of 524 and 4 975 individuals were sampled from Bio and Red
413 sediments, respectively, of which 35.5% and 4.2% were macrofauna *sensu stricto.*
414 On carbonate crusts, a total of 3 170 individuals were collected, among which 60.5%
415 were macrofauna *sensu stricto*.
416
417 Relative macrofaunal abundances varied between both soft-sediment microhabitats
418 (Bio and Red) and carbonate crusts and even between replicates of the same
419 microhabitat (Table 3). In bioturbated sediments, bivalves and polychaetes were the
420 dominant macrofaunal groups constituting 50% and 36% of the total abundance,
421 respectively. Other groups were present, but in much lower abundances (<5.4%,
422 Table 3). In the reduced sediments, all three replicates were very similar with a
423 dominance of polychaetes that represented a mean of about 96% of the total
424 macrofaunal abundance (Table 3). A few bivalves and gastropods were present.
425 Finally, all three carbonate crust replicates were similar in terms of composition, but
426 dominant taxa varied between samples. While CC1 and CC2 were dominated by
427 rissoid gastropods (*Laeviphitus verduini*, Van Aartsen et al., 1989, from 64.6 to
428 72.2%), CC3 was dominated by an undescribed species of mytilid bivalve (68.8%,
429 Table 3). These bivalves shared morphological similarities with Idas modioliformis
430 (Sturany, 1896) from the eastern Mediterranean Sea and a preliminary molecular
431 study suggests that they may belong to the Bathymodiolinae family and even
432 represent a new genus (Ritt et al. unpublished data). We also have molecular
433 evidence suggesting that this mytilid may harbour symbiotic bacteria (Ritt et al.
434 unpublished data). Cnidarians, polychaetes and crustaceans were also present on
435 CC but in lower abundances. The fauna found at the bottom of the combined-sample
436 box (CC_{box}) was largely dominated by rissoid gastropods (40.5%, Table 3).
437
438 Despite the large sieve mesh size used (250 µm), numerous meiofaunal specimens
439 were found in our samples (Table 4). When added to macrofauna, they contributed

from 17.7% to 98.3% of the total faunal abundance, with a lower impact in CC (Table 4). Nematodes were consistently the dominant taxon, representing >79% of the meiofauna (Table 4). Copepods were the second most dominant meiofaunal taxon in Bio and CC, but were absent in Red. Only a few ostracods were observed in soft-sediment microhabitats (<0.5%, Table 4).

Average macrofaunal densities varied from 3 433 ind./m² in Red, to 15 325 ind./m² in CC with an intermediate value of 9 300 ind./m² in Bio (Table 5). Compared to macrofauna, the meiofaunal density ranking showed the opposite trend with minimum densities in CC (10.4 ind./10 cm²) and maximum densities in Red (79.4 ind./10 cm²). They were intermediate in the Bio microhabitat (16.9 ind./10 cm², Table 5).

Rarefaction curves based on macrofaunal data (Figure 4a) show that the sampling effort was insufficient, especially in Bio (n=1) and Red (n=3). Nevertheless, the single sample from Bio had the highest taxonomic richness. For CC (n=3), the curve seems to level off, suggesting that most macrofaunal taxa was sampled (Figure 4a). However, the ranking of the three curves would probably remain the same with the addition of new macrofaunal samples and we can conclude with some confidence that the total taxonomic richness (S) was highest in Bio, lowest in Red and intermediate in CC (Figure 4a). Finally, the sharp increase of the Bio curves (Figure 4a) indicates that, with each additional individual sampled, the probability of it representing a new taxon was high. This pattern also demonstrates that Bio showed a more even taxon distribution than the two other microhabitats, a result that was confirmed by Pielou's index (*J*', Table 5). Meiofaunal samples were largely dominated by nematods (from 79 to 100%) that were not identified below the phylum level and most likely include several families and species. Hence, only family richness for copepods, ostracods and mites is reported in Table 5 as a measure of alpha-diversity.

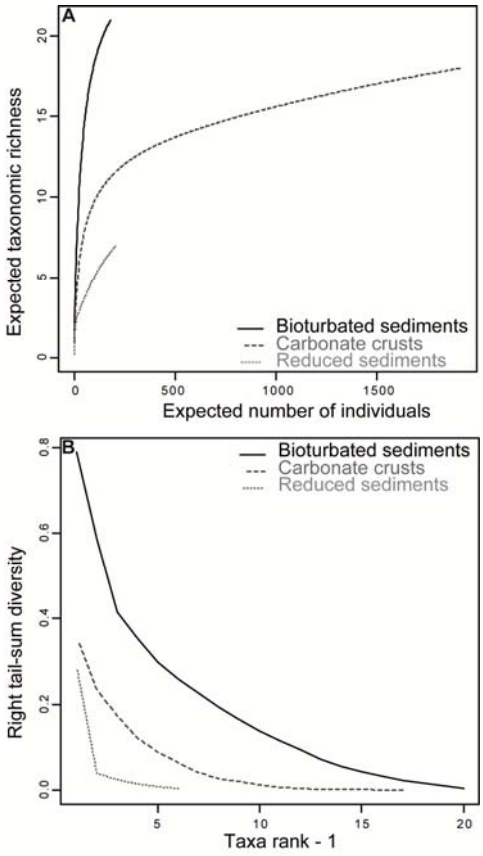

Fig. 4. Rarefaction curves (A) and right tail-sum (B) intrinsic diversity profiles according to the different microhabitats (MarNaut cruise, 2007). The CC_{Box} data were included.

The right tail-sum (RTS) intrinsic diversity profiles (Figure 4b) confirmed that Bio had the highest evenness. The Bio curve is positioned above the two others and the most abundant taxon represented only about 20% of the total macrofaunal abundance. In Red, the dominant taxon represented nearly 70% of macrofaunal abundances (Figure 4b). Classical diversity indices, and their numbers equivalents (Table 5), give the same alpha-diversity ranking. Classic diversity indices gave a consistent ranking (CC>Bio>Red; Table 5).

3.2.2. Symbiont-bearing fauna versus heterotrophic fauna

Symbiont-bearing fauna were present in various proportions in Bio and CC microhabitats, and totally absent in Red. Overall, they represented about 3.8% of the abundance in the Bio microhabitat, compared to 8.9 to 68.8% in CC. Symbiont-bearing fauna were represented by various bivalve families, including the Vesicomyidae, Lucinidae and Mytilidae. Live mytilids (adult and post-larvae) were only observed in CC (Table 3). However, dead specimens (post-larvae) were found

in large numbers in both soft-sediment microhabitats, reaching higher densities in Red. No data were available on the presence of symbiont-bearing fauna in the meiofaunal compartment.

3.2.3. Vertical distribution of the fauna within the sediments

The vertical distribution of the macrofauna varied among the two soft sediment microhabitats (Bio & Red, Figure 5a). Although the distribution pattern varied slightly between the three Red replicates, the macrofauna observed in Red was concentrated in the uppermost sediment layers with most (up to 80%) located within the top 3 cm (Figure 5a). In Bio, the fauna was more abundant in the very first layer (0-1 cm, 45%) and distributed more evenly among the others. Abundance reached minimum values below 10 cm in all samples (Figure 5a).

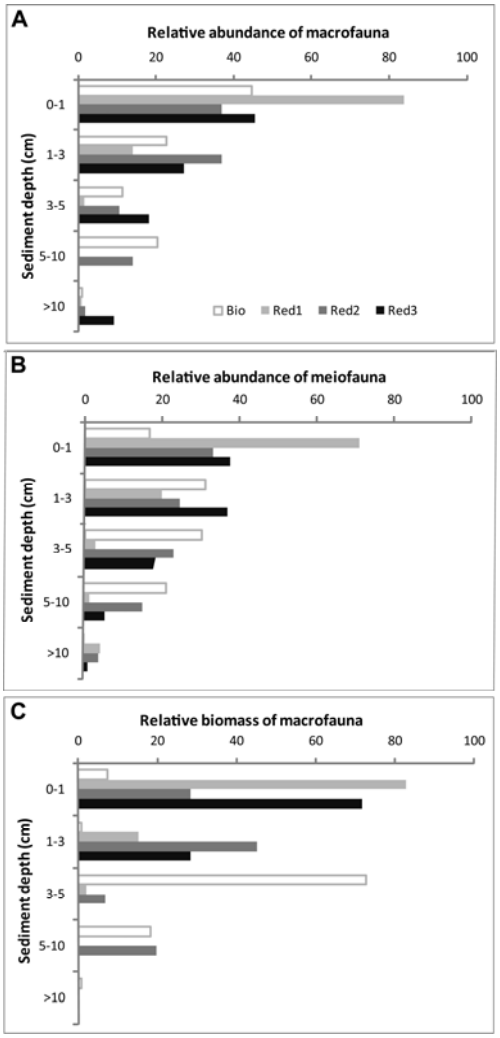

Fig. 5. Vertical distribution of (A) macrofaunal and (B) meiofaunal relative abundances and (C) relative biomass of macrofaunal taxa according to depth in the two soft-sediment microhabitats. Bio= bioturbated sediments, n=1; Red = reduced sediments, n=3.

Between 30 to 80% of meiofaunal abundance was observed in the first layers (0-1 cm) of Red and then decreased gradually with depth (Figure 5b). In Bio, the distribution of meiofauna reached higher abundances in the 1-5 cm sediment layers. Nematodes were present at all depths (even >10 cm) whatever the microhabitat, whereas copepod crustaceans were restricted to the upper 10 cm. As for macrofauna, meiofauna were rare in the deep sediment layer [>10 cm], they represented less than 5% of the total faunal abundance (Figure 5b).

3.2.4. Macrofaunal biomass

The highest macrofaunal biomass was found on CC reaching an average of 0.806 kg ww/m² (Table 5). Mytilids were the main contributors of this relatively high biomass. The biomass found at the bottom of the combined-sample box (CC_{box}), was negligible, only reaching 0.0033 kg. In the two other microhabitats, the mean biomass was 0.0018 kg ww/m² on Bio and 0.0019 kg ww/m² on Red (Table 5). The low values of biomass found in these microhabitats, compared to the crusts, were related to the presence of small organisms. Most of the biomass was found in the upper 5 cm of the sediments (Figure 5c). While it was mostly concentrated in the top 3 cm in Red, it was highest at 3-5 cm depth in the Bio microhabitat (Figure 5c).

3.2.5. Within and among microhabitat variation

Hierarchical clustering and PCA on macrofaunal abundances sensu stricto illustrate variations between the carbonate crusts and the two soft substratum microhabitats (Figure 6). The ordination clearly separates the three microhabitats along the two first axes that represent 77.4% of the total variance (Figure 6a). The three microhabitats are separated along the first axis, which contains 48% of the variance in the faunal variation. Inter-microhabitat variability was larger than intra-microhabitat variability as all replicate samples from Red and CC microhabitats grouped together. On the second axis, the Red and CC microhabitats grouped together while Bio stood alone. This axis explained 29.4% of the variance in the faunal variation (Figure 6a). In terms of structuring taxa, the rissoid gastropods *Laeviphitus verduini* and the dorvilleid polychaetes contributed significantly to the two first axes, characterizing the CC microhabitat and the Red microhabitat, respectively (Figure 6a). Other taxa, such as the mytilid bivalves, were important, but to a lesser extent, in the positioning of the microhabitats on the two first axes (Figure 6a).

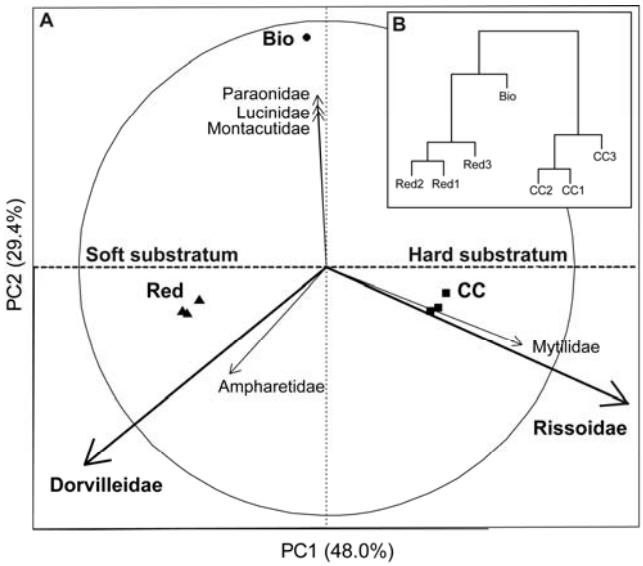

Fig. 6. (A) Ordination graph (PCA, scaling type 1) with the circle of equilibrium contribution (radius=0.77) and the two first axes representing 77.4% of the total variance. Vectors shorter than 0.42 were removed. (B) Ward's hierarchical clustering performed with Hellinger-transformed macrofaunal abundances of high taxonomic level data for each microhabitat type, Bio = bioturbated sediments, Red = reduced sediments, CC = carbonate crust.

Interestingly, a PCA with Hellinger transformed meiofaunal data only (not shown) exhibited the same general distance patterns as the one with macrofauna *sensu stricto* (Procruste Test stat=0.83, p=0.006, 1000 permutations). However, meiofauna sampling was very incomplete, especially on hard substratum, and these results might reflect this paucity of observations.

The three microhabitats could also be distinguished when considering only the polychaetes at the family level. Most families observed in the Bio microhabitat were absent in Red and vice versa (Table 3). Moreover, while at least eight families were present in the single Bio sample, and seven in CC, only four were observed in the three Red samples (Table 3). Siboglinid polychaetes were absent from our samples and were not observed in the seep areas that we explored in the Marmara Sea. Multivariate analysis performed on just the polychaete family abundances also separated the microhabitats along the two first axes, representing 79.3% of the total variance (Figure 7a). Bio was clearly distinct from Red and CC along the first axis, which explained 59.6% of the variance whereas the distinction along the second axis was not as clear (Figure 7a). Paraonidae and Dorvilleidae were the most important taxa in structuring the position of samples in the ordination. Cirratulidae, Hesionidae

and Ampharetidae also had an important contribution on the second axis. Ward's hierarchical clustering corroborated this separation (Figure 7b). However, no clear distinction between the polychaete composition in CC and Red was established.

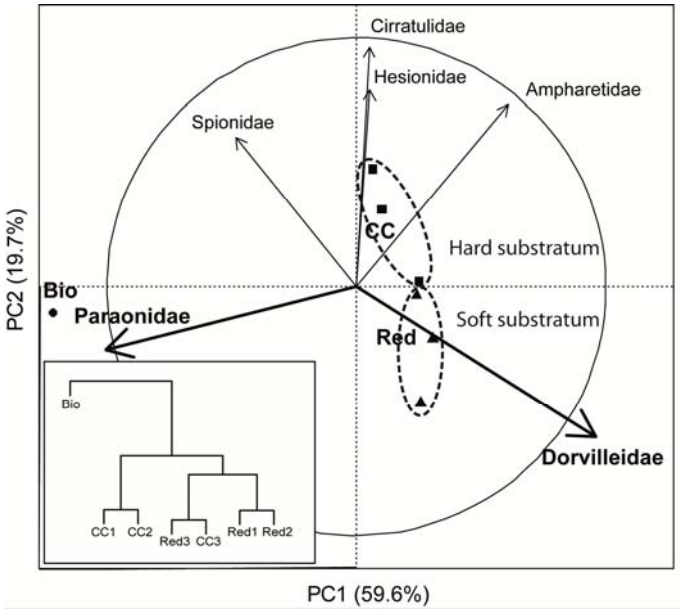

Fig. 7. (A) Ordination graph (PCA, scaling type 1) with the circle of equilibrium contribution (radius=0.72) and the two first axes representing 79.3% of the total variance. Vectors shorter than 0.56 were removed. (B) Ward's hierarchical clustering performed with Hellinger-transformed abundances of polychaete families data for each microhabitat type, Bio = bioturbated sediments, Red = reduced sediments, CC = carbonate crust. The possible link between the second axis and substratum type is noted.

The environmental and faunal results suggest a model of fluid circulation (Figure 8) that relates faunal composition and their patchy distribution to the flux of low-chlorinity fluid emissions. The upward flux was hypothesized to be higher under the Red microhabitat and lower under the Bio and CC microhabitats, where symbiont-bearing bivalves, vesicomyids and mytilids, respectively, were living. Thus, these taxa appear to be reliable indicators of the presence of chemical fluxes, especially sulphides, at the sediment-water interface.

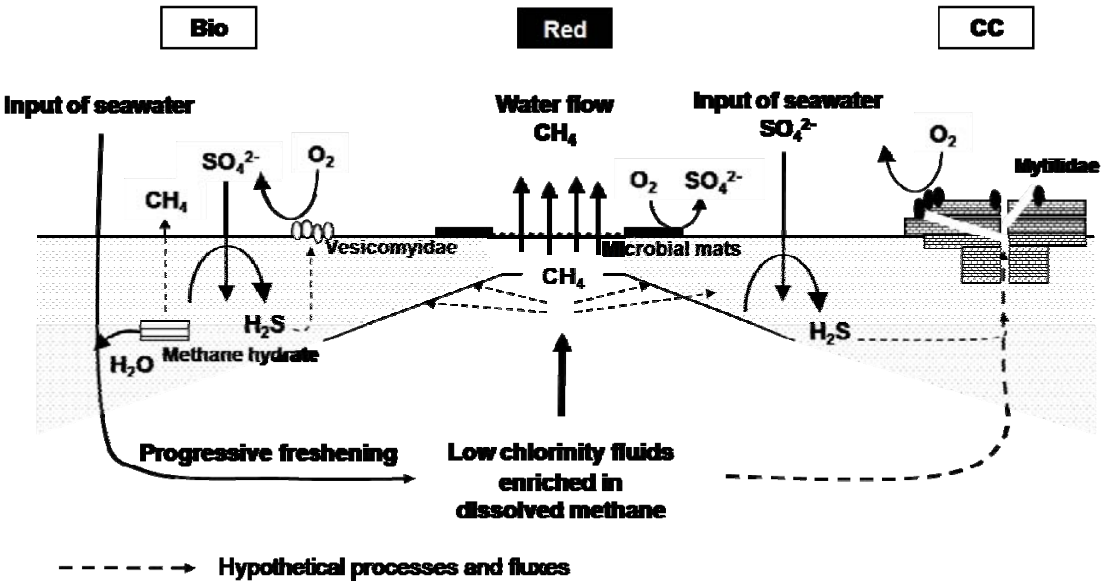

Fig. 8. Schematic hypothetical representation (modified from Henry et al., 1996 and Olu et al., 1996) of physical and chemical processes in the first few centimetres of sediments at each microhabitat type, Bio = bioturbated sediments, Red = reduced sediments, CC = carbonate crust. Doted line = hypothetical processes and fluxes. The distance between microhabitats is not drawn to scale.

571

572 ## 4. Discussion

573 ### 4.1. Environmental conditions in the Marmara Sea

574 The cold seeps of Marmara Sea illustrate an example of an active margin setting with
575 low-chlorinity upward fluids. Contrary to other seep sites, the regions of the Marmara
576 Sea explored in this study did not reveal spectacular evidence of fluid emissions on
577 the seafloor, such as mud volcanoes, pockmarks or brine pools (Milkov, 2000;
578 Hovland et al., 2002; Judd and Hovland, 2007). Instead, fluid fluxes appeared to be
579 unevenly distributed along active faults where fractures allow released gas to escape
580 or to filter through sediments (Geli et al., 2008; Zitter et al., 2008). Thermogenic
581 methane-rich bubble emissions occur (Bourry et al., 2009) and brackish water can be
582 expelled through chimneys on the seafloor (Zitter et al., 2008). Furthermore, black
583 patches (reduced sediments) throughout the different basins have been observed
584 within the larger Çinarcik basin where the dissolved oxygen concentration is the
585 lowest. In fact, a gradient of dissolved oxygen in the water column is observed from
586 the western to the eastern basins with concentrations reaching 50 µmol/kg in the
587 Tekirdag basin, 25 µmol/kg in the Central basin and 8 µmol/kg in the Çinarcik basin
588 (Lionel Finchel, INSU). The Marmara Sea is not as anoxic as the Black Sea, but
589 pollution in the Marmara Sea due to anthropogenic activities (Cetecioglu et al., 2009)
590 and the proximity of land lead to high inputs of organic matter that can reach the
591 seafloor, enhancing microbial activity and organic matter degradation there. This is

supported by the observation of huge fluxes of marine snow during diving, even in the deeper part of the Central basin at depths of up to 1200 m.

Tectonic processes appear to play a major role in the occurrence of fluid emissions in this region and their highly dynamic nature may induce high spatial and temporal variation that may in turn influence faunal distribution (Zitter et al., 2008). This high spatial heterogeneity was apparent in the Red microhabitat, where replicates separated by only a couple of meters varied by as much as five fold in methane concentrations. The chemical data at the sediment-water interface (i.e. methane) as well as in pore water (i.e. sulphates, oxygen) confirmed the presence of fluid emission and provided evidence for seawater convection between the two soft-sediment microhabitats. Despite the incompleteness of our environmental factor dataset and the large within-microhabitat variations observed, our data suggest that both soft sediment microhabitats had a distinct chemical signature.

4.2. Microhabitat characteristics

4.2.1. Bioturbated sediment microhabitat

The Bio microhabitat was characterised by deeper oxygen and sulphate penetration. We can assume that the penetration of these elements in the sediments is favoured by the presence of burrows, probably built by crustaceans. It has been shown that complex burrows may influence the overall sedimentology and geochemistry of the seafloor and especially oxygen penetration (Aller, 1988; Ziebis et al., 1996). The jagged chlorinity profile can be interpreted as the consequence of transient diffusion-advection resulting from bio-irrigation. The sulphate concentrations remained relatively high and, with the exception of the lowest point at 16-18 cm depth, were compatible with mixing between seawater and a fluid of 100 mmol/l chlorinity and 0 mmol/l sulphate, representative of fossil pore water originating from the ancient Marmara lake (Zitter *et al.*, 2008). The top of the sulphate reduction zone lays 16 cm below the seafloor and likely to the end of the bio-irrigated zone. This type of system has already been observed at Nankai (Henry et al., 1992; Toki et al., 2004) or on the Barbados Trench (Henry et al., 1996), as explained below for the Red microhabitat.

The observed taxonomic richness was highest in the Bio microhabitat, even though only a single sample was collected. This microhabitat had intermediate macrofaunal

626 densities and was dominated by bivalves — especially Montacutidae and
627 Vesicomyidae —, polychaetes and nematodes. It is interesting to note that the
628 vesicomyid Isorropodon *perplexum* (Sturany, 1896) and another symbiont-bearing
629 species, the lucinid *Lucinoma kazani* (Salas and Woodside, 2002) have only been
630 observed at Mediterranean Sea cold seeps where they are fuelled by the Anaerobic
631 Oxydation of Methane (AOM) that induces H_2S production (Boetius et al., 2000).
632 Vesicomyidae beds have already been observed at numerous cold seep sites with
633 higher densities such as that around the centre of the Atalante mud volcano where
634 they reach up to 10 ind./m² (Olu et al., 1996), or at the Nankai Trench where they
635 reach 1 000 ind./m² (Henry et al., 1992). Vesicomyid and lucinid densities in Bio were
636 much lower with up to 200 and 150 ind./m² respectively, but their presence was not
637 only an indication of fluid venting but also of shallow sulphide production in this
638 microhabitat. Both families are known to live half-buried in the sediments where they
639 are able to extend their foot to capture sulphide (Barry and Kochevar, 1998;
640 Wallmann et al., 1997). As supposed by the diffusion-advection model, the sulphide
641 production in Bio may occur deep within sediments.
642
643 4.2.2. Reduced sediment microhabitat
644 The presence of methane at the interface of reduced sediment was the main
645 evidence of seepage activity at the study site. This microhabitat was also
646 characterised by low dissolved oxygen concentrations at the water-sediment
647 interface and the sulphate profiles showed a sharp decrease in the first 10 cm.
648 However, contrary to dissolved oxygen, we cannot assume that sulphates decreased
649 only by simple consumption in sediments. The model based on chlorinity profiles
650 supported the hypothesis that the Red microhabitat corresponded to a zone of fairly
651 uniform Darcian flow (i.e. within fluid velocities ranging 0.5-0.75 m/yr) for a fluid of
652 constant chlorinity (496 mmol/l) and containing no sulphates. The ascending fluid
653 appears to be a mix of seawater and brackish pore fluid that dilutes the chloride. In
654 fact, the salinity of the brackish pore fluids contained in the Marmara Sea sediments
655 a few tens of meters below the seafloor is only about 100 mmol/l (Zitter et al., 2008).
656 This mixing model implies that convection occurs around the brackish springs at a
657 larger scale (1-100 m) than the one investigated here. Hydrate dissociation may also
658 explain the progressive freshening of seawater within sediments in seeps.
659 Nevertheless, no gas hydrates were found in our samples, although they do occur in

660 different basins of the Marmara Sea where the conditions of pressure and
661 temperature corresponded to the hydrate stability zone (Bourry et al., 2009).
662
663 According to the proposed fluid circulation model, the Red microhabitat was
664 dominated by advective fluxes (0.4-0.8 m/yr) that were sufficient to inhibit inflow and
665 to extend the sulphate reduction to the sediment surface. Hence, the depth at which
666 sulphate penetrated into the sediments did not appear to be controlled by reaction
667 rates but rather by competition with molecular diffusion in the vigorous ascending
668 fluid flow. More sophisticated modelling would be required to determine actual
669 reaction rates. Similar geochemical processes were also observed at the Nankai
670 Trench (Henry et al., 1992; Toki et al., 2004) and at the Barbados accretionary
671 prisms (Henry et al., 1996), two sites also characterised by low chlorinity upward
672 fluxes.
673
674 In terms of fauna, the Red microhabitat was characterised by low taxonomic
675 diversity, the absence of symbiont-bearing fauna, the lowest macrofaunal densities
676 and the large dominance of two ubiquitous polychaete families: the non-sedentary
677 Dorvilleidae and the tube-building Ampharetidae. These two families are typical of
678 areas enriched in organic matter (Fauchald and Jumars, 1979). The presence of low-
679 diversity polychaete assemblages, dominated by one or two families, has been
680 already observed in microbial mats from the Eel River basin, Hydrate Ridge and Gulf
681 of Mexico (Levin et al., 2003; Sahling et al., 2002; Robinson et al., 2004). In our
682 study, Ampharetidae were the second-ranked polychaete taxa. Members of this
683 family have been observed in large numbers at other reduced sediments sites such
684 as at the Hikurangi Margin (New Zealand) where they reach a density of up to 72 000
685 ind./m² (Sommer et al., 2009b). This site lies on an active margin at a depth similar to
686 our study site (~ 1050 m) with high concentrations of dissolved oxygen and methane
687 at the water-sediment interface (197 µmol/l and 1 962 µmol/l, respectively; Table 6).
688 In our study, dorvilleid and ampharetid polychaetes may represent the main
689 consumers of dissolved oxygen at the surface of the Red microhabitat and account
690 for the low oxygen concentration, which never exceeded 51 µmol/l.
691
692 Meiofaunal densities, dominated by nematodes, were highest in the Red
693 microhabitat, four times as great as those observed in the two other microhabitats.

They were higher (from 1 058 to 134 800 ind./m²) than those observed in the Black Sea at shallower depth (250 m, from 2 397 to 52 593 ind./m², Sergeeva and Gulin., 2007). Nevertheless, our meiofaunal densities were much lower than those observed on the Atalante mud volcano at the Barbados accretionary prism where nematode density reaches up to 8 300 000 ind./m² (Olu et al., 1997). However, the large sieve size used (250 µm) lead to the underestimation of meiofaunal density in our study. The low similarity between replicates mostly reflected the differences in abundance due to the high spatial heterogeneity of meiofauna, but also to the sampling strategy used.

4.2.3. Carbonate crust microhabitat

Carbonate crusts are known to be formed in reducing environments with methane inputs being oxidized by micro-organisms involved in the AOM (Aloisi et al., 2002; Aloisi et al., 2000). However, their immediate environment may change after they have formed. The carbonate crusts sampled here occur as a cm-thick layer that covers a meter-high mound covered by sediments; this structure may be considered as chemoherms (Teichert et al., 2005) that are built by fluid flow and/or escape of free methane gas into the water column. The crust is composed of magnesian calcite that was the product of anaerobic oxidation of methane as evidenced by the very low $\partial^{13}C$ value. However, additional chemical data will be necessary to gain a better understanding of this microhabitat and to position it within the gradient of environmental conditions observed in the two other microhabitats.

In terms of fauna, the CC microhabitat was characterized by intermediate diversity, the highest biomass and the highest macrofaunal densities, largely dominated by rissoid gastropods and by symbiont-bearing mytilids. The CC microhabitat exhibited the highest proportion of symbiont-bearing fauna and the occurrence of the latter was evidence of sufficient fluid flow and of exchanges between seawater and sediments to sustain symbiotic processes. Furthermore, this microhabitat harboured the highest percentage of symbiont-bearing fauna represented by mytilids that constitute the major part of the total biomass. Like *Idas sp.* from the Nile deep-sea fan, that lives in association with up to six different microbial symbionts (Duperron et al., 2008), the new mytilid species found in the Marmara Sea may harbour both thiotrophic and methanotrophic endosymbionts. To date our preliminary analyses only confirm the

728 presence of thiotrophic endosymbionts (Ritt et al. unpublished data). As on the giant
729 pockmark off West Africa (Olu-Le Roy et al., 2007), carbonate crusts with mytilids
730 appear to be under the influence of high fluid flow, higher than in sediments with
731 vesicomyids, but lower than in reduced sediments in our study case (Table 6).
732
733 4.3. Comparison between microhabitats (at the local scale)
734 Multivariate analyses showed a first distinction between communities found on hard
735 and soft substratum microhabitats. The second axis could be related to a gradient of
736 seepage influence (methane, oxygen and possibly sulphide). However, our chemical
737 dataset was insufficient to establish statistical links between faunal distribution and
738 environmental conditions and additional sampling would be necessary to further
739 explore this hypothesis. The two distinct sediment microhabitats were characterized
740 by contrasting methane supply and, probably, sulphide production. The Red
741 microhabitat was dominated by upward advection of pore fluid that causes strong
742 chemical gradients in the first few cm. At the Bio microhabitat, the production of
743 hydrogen sulphide probably occurs below the bioturbated layer and is most likely
744 controlled by bioirrigation fluxes (Wallmann et al., 1997). While the strong chemical
745 gradients at Red can be exploited by free-living bacteria, more complex species
746 interactions such as symbiosis could become advantageous at a site where sulphide
747 production and oxygen supply are separated by at least 15 cm, as in Bio. Sulphide-
748 tolerant polychaetes and nematodes lived on the surface of Red, whereas symbiont-
749 bearing fauna, such as Vesicomyidae bivalves, were more evenly distributed and
750 buried in Bio. The distribution patterns observed in our study support the hypothesis
751 voiced by other authors suggesting that Ampharetidae and Dorvilleidae have a higher
752 tolerance to sulphides (Levin et al., 2003; Sahling et al., 2002). Focusing only on
753 polychaete families gives a different portrait. First of all, within-microhabitat variations
754 appear to be proportionally more important than when considering the entire
755 community. Also, Bio comes out as markedly different from all the others and the
756 distinction between hard and soft substratum communities almost disappears.
757
758 These observations indicate that the faunal distribution at the Marmara Sea seeps is
759 patchy and somewhat linked to the nature of the substratum and physico-chemical
760 conditions that constrain the composition of the assemblages. Thus, within the same
761 type of substratum (soft sediments), fluid flow velocities and chemical gradients such

762 as methane, oxygen and possibly sulphide concentrations appear to play a role in
763 faunal composition.
764
765 4.4. Comparison between microhabitats (at the global scale)
766 A total of 60 taxa, including meiofauna, were identified at our study site among which
767 8 were also observed at eastern Mediterranean sites so far (Olu-Le Roy et al., 2004).
768 This suggests that exchanges between the eastern Mediterranean Sea and the
769 Marmara Sea seep sites continue to occur or occurred in the past. However,
770 Siboglinidae polychaetes were not observed, neither during the MARMARASCARPS
771 cruise (Zitter et al., 2008), nor during our cruise. This is surprising since siboglinids
772 are present at most Mediterranean seep sites studied (Olu-Le Roy et al., 2004; Ritt et
773 al., in prep.). This may simply be due to the lack of sampling in this area. In fact, a
774 siboglinid tube was found at 1000 m depth during a recent Turkish cruise in 2008 (L.
775 Artüz, pers. com.). Another hypothesis is that the geographic barrier induced by the
776 Dardanelle sill (70 m) may have limited siboglinid larval dispersion within the
777 Marmara Sea but only additional sampling will help resolve this conundrum.
778
779 The flow velocity observed at our study site (0.4-0.8 m/yr) was much lower than
780 those previously reported in the Nankai Trough accretionary wedge (Henry et al.,
781 1992), the Cascadia subduction zone or the Peru continental margin (Linke et al.,
782 1994), all of which fall into a much larger range of 10-1 000 m/yr. These high rates
783 are probably due to the combination of different factors, such as the geological
784 setting, the presence of active thrusts, and the permeability of sediment layers
785 (Henry et al., 2002). Furthermore, the distribution of the faunal communities in the
786 Marmara Sea appears to differ from some large seep sites where a zonation of
787 faunal communities has been observed at the 100 m to km scale (Le Pichon et al.,
788 1990; Olu et al., 1996). This kind of ecological zonation has already been observed
789 at larger scale on the Atalante mud volcano (Olu et al., 1996), the Håkon Mosby mud
790 volcano (Niemann et al., 2006b), or the Hydrate Ridge (Sahling et al., 2002). The
791 centre of the Atalante mud volcano is controlled by high fluid flux and colonised by
792 high densities of nematodes, whereas clam beds are observed on the “Ridge zone”,
793 where the upward flux is lower. At the Håkon Mosby mud volcano, the active centre
794 is only colonized by meiofaunal organisms, fauna form concentric belts around the
795 active centre of the mud volcano (Jerosch et al., 2006) and this faunal distribution

appears to be directly related to chemical gradients (Jerosch et al., 2006; Niemann et al., 2006b). At Hydrate Ridge, the flux under microbial mats is controlled by the dissociation of gas hydrate and the abiotic conditions are much harsher (30 mmol/l sulphide) than within the surrounding sediments where the clams beds are found (Sahling et al., 2002). At sites such as the Hydrate and Blake ridges, changes in the faunal composition are linked to smaller spatial scales (Sahling et al., 2002; Van Dover et al., 2003). There, microbial mats colonise hydrate deposits with high sulphide concentrations; they are surrounded by vesicomyid beds and, further away, by solemyid beds, following a gradient in sulphide concentrations. The faunal distribution in the Marmara Sea appears to be characterised by similar small-scale patterns. Patches of reduced sediments were dominated by ampharetid and dorvilleid polychaetes and nematodes surrounded by microbial mats and the entire area was also surrounded by more highly oxygenated sediments colonised by Vesicomyidae and Lucinidae symbiont-bearing bivalves.

On soft sediments, the faunal distribution seems strongly reliant on sulphide production, which relies on the intensity of fluid flow. Indeed, a biological zonation was observed along a sulphide concentration gradient related to the occurrence of gas hydrates on the Cascadia margin (Sahling et al., 2002). Likewise, on the Håkon Mosby mud volcano, fluid flux gradient was related to faunal distribution patterns from the centre to the periphery (Niemann et al., 2006b). Methane concentrations measured above reduced sediments (Red, from 0.14 to 0.70 µmol/l) match the lowest ranges observed at other seep sites (Table 6). Indeed, measured methane concentrations above seep faunal assemblages within reduced sediment microhabitats range from 0.14 µmol/l (this study) to 1 962 µmol/l on the New Zealand margin (Sommer et al., 2009b, Table 6). Sediments filled with gas hydrates (and microbial mats) show the highest methane concentrations of all with concentrations of up to 6 500 µmol/l (Table 6). Methane has been shown to influence the distribution of the fauna at other seep sites (Olu et al. 1997, Olu-Le Roy et al. 2007, Sergeeva and Gulin al., 2007).

Carbonate crusts may constitute an intermediate environment in terms of chemical gradients, and probably fluid intensity in the Marmara Sea, whereas they appear to

be associated with highest methane concentrations and probably highest fluid flow at the Regab pockmark (Olu-Le Roy et al., 2007).

4.5. Conclusion and perspective

The Red microhabitat showed low taxonomic diversity and was dominated by surface deposit-feeders, whereas the Bio microhabitat harboured symbiont-bearing, burrowing species. In addition to chemical measurements and models based on them, we deduce that the Red microhabitat was influenced by fluids that prevent the establishment of non-tolerant species or even symbiotic species. On the other hand, Bio was also influenced by fluids but to a lesser extent, allowing an increase in diversity in association with an increase in trophic complexity and specialisation (i.e. symbioses). Interestingly, the CC microhabitat may sustain up to 69% of symbiont-bearing fauna and especially mytilids, suggesting that fluid-flux exchanges between seawater and sediments are high enough to sustain symbiotic processes. These hard substratum microhabitats would be characterised by intermediate environmental conditions, harbouring higher biomass and densities and intermediate diversity. Additional sampling will be necessary to further explore the links between faunal distribution and environmental conditions in the Marmara Sea and to validate the proposed model.

We will soon complete the molecular phylogeny and morphological description of the new mytilid found on the Marmara carbonate crusts. Thus, our preliminary results suggested, that even though this species shared morphological similarities with *Idas modioliformis* (Sturany, 1896) from the eastern Mediterranean Sea, it may represent a new genus in the Bathymodiolinae family (Ritt et al. unpublished data). In addition, further analyses will be done to confirm the status of the bacteria as symbionts, visualize their distribution in the gills and define their nutritional role in this bivalve species.

Finally, adequate and representative sampling of the meiofaunal and microbial compartments, their activities and their trophic interactions as well as a complete environmental charaterization would be helpful in understanding the fine structure and functioning of the seep communities found in the Marmara deep basins.

5. Acknowledgments

Captains and crew of R/V *Atalante* as well as *Nautile*'s pilots are warmly acknowledged for their dedicated assistance and for contributing to the success of the cruise, especially dive 1665. We thank Patricia Pignet for her valuable help with the chemical analyses. The faunal samples were identified by a network of taxonomists from the Muséum National d'Histoire Naturelle of Paris (France), the German Centre for Marine Biodiversity Research (Germany), the University of Lodz (Poland), the Russian Academy of Sciences of Moscow, the Kamchatka Branch of the Pacific Institute of Geography of Petropavlovsk-Kamchatsky and the Institute of Marine Biology of Vladivostok (Russia). The English was professionally edited by Carolyn Engel-Gautier. BR's thesis was funded by Ifremer. This research project benefited from funds from the HERMES and HERMIONE European projects (contract # 511234 and #226354) as well as ANR DEEP-OASES (ANR06BDV005) and from support from the GDR ECCHIS.

6. References

Aharon, P., Fu, B.S., 2003. Sulfur and oxygen isotopes of coeval sulphate-sulfide in pore fluids of cold seep sediments with sharp redox gradients. Chemical Geology 195 (1-4), 201-218.

Aller, R.C., 1988. Benthic Fauna and Biogeochemical Processes in Marine Sediments: the Role of Burrow Structures. In: Blackburn, T.H., Sorensen, J. (Eds.), Nitrogen Cycling in Coastal Environments. John Wiley & Sons Ltd, pp. 301-329.

Aloisi, G., Bouloubassi, I., Heijs, S.K., Pancost, R.D., Pierre, C., Damste, J.S.S., Gottschal, J.C., Forney, L.J., Rouchy, J.M., 2002. CH4-consuming microorganisms and the formation of carbonate crusts at cold seeps. Earth and Planetary Science Letters 203 (1), 195-203.

Aloisi, G., Pierre, C., Rouchy, J.M., Foucher, J.P., Woodside, J., 2000. Methane-related authigenic carbonates of eastern Mediterranean Sea mud volcanoes and their possible relation to gas hydrate destabilisation. Earth and Planetary Science Letters 184 (1), 321-338.

Alpar, B., 1999. Underwater signatures of the Kocaeli Earthquake (August 17th 1999). Turkish Journal of Marine Sciences 5, 111-130.

Ambraseys, N.N., 2000. The seismicity of the Marmara Sea area 1800-1899. Journal of Earthquake Engineering 4 (3), 377-401.

Ambraseys, N.N., Finkel, C.F., 1991. Long-terme seismicity of Istanbul and of the Marmara Sea region. Terra Nova 3 (5), 527-539.

Ansal, A., Akinci, A., Cultrera, G., Erdik, M., Pessina, V., Tonuk, G., Ameri, G., 2009. Loss estimation in Istanbul based on deterministic earthquake scenarios of the Marmara Sea region (Turkey). Soil Dynamics and Earthquake Engineering 29 (4), 699-709.

Armijo, R., Flerit, F., King, G., Meyer, B., 2004. Linear elastic fracture mechanics explains the past and present evolution of the Aegean. Earth and Planetary Science Letters 217 (1-2), 85-95.

Armijo, R., Pondard, N., Meyer, B., Ucarkus, G., de Lepinay, B.M., Malavieille, J., Dominguez, S., Gustcher, M.A., Schmidt, S., Beck, C., Cagatay, N., Cakir, Z., Imren, C., Eris, K., Natalin, B., Ozalaybey, S., Tolun, L., Lefevre, I., Seeber, L., Gasperini, L., Rangin, C., Emre, O., Sarikavak, K., 2005. Submarine fault scarps in the Sea of Marmara pull-apart (North Anatolian Fault): implications for seismic hazard in Istanbul. Geochemistry Geophysics Geosystems 6, 29.

Artemov Yu. G., Egorov V.N., Polikarpov G.G., Gulin S.B., 2007. Methane emission on the hydro-and atmosphere by gas bubble streams in the Dniper paleo-delta, the Black Sea. Marine Ecological Journal 6 (3), 5-26.

Barry, J.P., Kochevar, R.E., 1998. A tale of two clams: differing chemosynthetic life styles among vesicomyids in Monterey Bay cold seeps. Cahiers De Biologie Marine 39 (3-4), 329-331.

Bayon, G. Loncke, L. Dupre, S., Ducassou, E., Duperron, S., Etoubleau, J., Foucher, J.P., Fouquet, Y., Gontharet, S., Huguen, C., Klaude, I., Mascle, J., Olu_Le Roy, K., Ondreas, H., Pierre, C., Sibuet, M., Stadnistskaia, A., Woodside, J., 2009. Multi-disciplinary investigations of fluid seepage on an unstable margin: the case of the Central Nile deep-sea fan. Marine Geology 261, 92-104.

Bergquist, D.C., Fleckenstein, C., Knisel, J., Begley, B., MacDonald, I.R., Fisher, C.R., 2005. Variations in seep mussel bed communities along physical and chemical environmental gradients.

Bergquist, D.C., Ward, T., Cordes, E.E., McNelis, T., Howlett, S., Kosoff, R., Hourdez, S., Carney, R., Fisher, C.R., 2003. Community structure of vestimentiferan-generated habitat islands from Gulf of Mexico cold seeps. Journal of Experimental Marine Biology and Ecology 289 (2), 197.

Berner, R.A., 1974. Kinetic models for the early diagenesis of nitrogen, sulfur, phosphorus and silicon in anoxic marine sediments. In: Goldberg, E.D. (Ed.), Marine chemistry. The Sea: ideas and observations on progress in the study of the seas, pp. 427-450.

Boetius, A., Ravenschlag, K., Schubert, C.J., Rickert, D., Widdel, F., Gieseke, A., Amann, R., Jorgensen, B.B., Witte, U., Pfannkuche, O., 2000. A marine microbial consortium apparently mediating anaerobic oxidation of methane. Nature 407 (6804), 623-626.

Bourry, C., Chazallon, B., Charlou, J.L., Pierre Donval, J., Ruffine, L., Henry, P., Geli, L., Çagatay, M.N., Inan, S., Moreau, M., 2009. Free gas and gas hydrates from the

940 Sea of Marmara, Turkey: chemical and structural characterization. Chemical Geology
941 264 (1-4), 197-206.

942 Campbell, K.A., 2006. Hydrocarbon seep and hydrothermal vent paleoenvironments
943 and paleontology: past developments and future research directions.
944 Palaeogeography Palaeoclimatology Palaeoecology 232 (2-4), 362-407.

945 Cavanaugh, C.M., 1983. Symbiotic Chemoautotrophic Bacteria In Marine-
946 Invertebrates From Sulfide-Rich Habitats. Nature 302 (5903), 58-61.

947 Cetecioglu, Z., Ince, B.K., Kolukirik, M., Ince, O., 2009. Biogeographical distribution
948 and diversity of bacterial and archaeal communities within highly polluted anoxic
949 marine sediments from the Marmara Sea. Marine Pollution Bulletin 58 (3), 384-395.

950 Childress, J.J., Fisher, C.R., Brooks, J.M., Kennicutt, M.C., II, Bidigare, R., Anderson,
951 A.E., 1986. A methanotrophic marine molluscan (Bivalvia, Mytilidae) symbiosis:
952 Mussels fueled by gas. Science 233, 1306-1308.

953 Craig, H., 1957. Isotopic standards for carbon and oxygen and correction factors for
954 mass-spectrometric analysis of carbon dioxide. Geochimica. et Cosmochimica. Acta
955 12, 133-149.

956 Dimitrov, L.I., 2002. Mud volcanoes - the most important pathway for degassing
957 deeply buried sediments. Earth-Science Reviews 59 (1-4), 49-76.

958 Dubilier, N., Bergin, C., Lott, C., 2008. Symbiotic diversity in marine animals: the art
959 of harnessing chemosynthesis. Nature Reviews Microbiology 6 (10), 725-740.

960 Duperron, S., Halary, S., Lorion, J., Sibuet, M., Gaill, F., 2008. Unexpected co-
961 occurrence of six bacterial symbionts in the gills of the cold seep mussel Idas sp
962 (Bivalvia : Mytilidae). Environmental Microbiology 10 (2), 433-445.

963 Egorov, V.N., Luth, U., Luth, C., Gulin, M.B., 1998. Gas seeps in the submarine
964 Dniper Canyon Black Sea: acoustics, video and trawl data. In: Luth U., Luth C., Thiel
965 H. (Eds), MEGASEEPS-Methane Gas Seeps Exploration in the Black Sea. Berichte
966 aus dem Zentrum fu.r Meeres- und Klimatoforsch, Hamburg:14, 11-21.

967 Fauchald, K., Jumars, P.A., 1979. The diet of worms: a study of polychaete feeding
968 guilds. Oceanography and Marine Biology Annual Review 17, 193-284.

969 Fisher, C.R., 1990. Chemoautotrophic And Methanotrophic Symbioses In Marine-
970 Invertebrates. Reviews in Aquatic Sciences 2 (3-4), 399-436.

971 Gage, J.D., 2003. Food inputs, Utilization, Carbon Flow and Energetics. Ecosystems
972 of the Deep Oceans. Elsevier Science BV, pp. 313-380.

973 Gauthier, O., Sarrazin, J., Desbruyeres, D., 2010. Measure and mis-measure of
974 species diversity in deep-sea chemosynthetic communities.

975 Geli, L., Henry, P., Zitter, T., Dupre, S., Tryon, M., Cagatay, M.N., de Lepinay, B.M.,
976 Le Pichon, X., Sengor, A.M.C., Gorur, N., Natalin, B., Ucarkus, G., Oezeren, S.,
977 Volker, D., Gasperini, L., Burnard, P., Bourlange, S., 2008. Gas emissions and active

tectonics within the submerged section of the North Anatolian Fault zone in the Sea of Marmara. Earth and Planetary Science Letters 274 (1-2), 34-39.

Gini, C., 1912. Variabilità e Mutabilità. Tipographia di Paolo Cuppini, Bologna.

Gonfiantini, R., Stichler, W., Kozanski, K., 1995. Standards and intercomparison materials distributed by the International Atomic Energy Agency for stable isotope measurements. in: Reference and Intercomparison Materials for Stable Isotopes of Light Elements, IAEA-TECDOC-825, IAEA, Vienna, 13-29.

Gontharet, S., Pierre C., Blanc-Valleron, M.M., Rouchy, J.M., Fouquet, Y., Bayon, G., Foucher, J.P., Woodside, J., Mascle, J., and the NAUTINIL Scientific Party, 2007. Nature and origin of diagenetic carbonate crusts and concretions from mud volcanoes and pockmarks of the Nile deep-sea fan (eastern Mediterranean Sea). Deep Sea Research II 54, 1292-1311.

Gotelli, N.J., Colwell, R.K., 2001. Quantifying biodiversity: procedures and pitfalls in the measurement and comparison of species richness. Ecology Letters 4 (4), 379-391.

Halbach, P., Holzbecher, E., Reichel, T., Moche, R., 2004. Migration of the sulphate-methane reaction zone in marine sediments of the Sea of Marmara - can this mechanism be tectonically induced? Chemical Geology 205 (1-2), 73-82.

Hecker, B., 1985. Fauna from a cold sulfur-seep in the Gulf of Mexico: comparison with hydrothermal vent communities and evolutionary implications. Bulletin of the Biological Society of Washington 6, 465-473.

Henry, P., Foucher, J.P., Le Pichon, X., Sibuet, M., Kobayashi, K., Tarits, P., Chamotrooke, N., Furuta, T., Schultheiss, P., 1992. Interpretation Of Temperature-Measurements From The Kaiko-Nankai cruise - modeling Of Fluid-Flow In Clam Colonies. Earth and Planetary Science Letters 109 (3-4), 355-371.

Henry, P., Lallemant, S., Nakamura, K., Tsunogai, U., Mazzotti, S., Kobayashi, K., 2002. Surface expression of fluid venting at the toe of the Nankai wedge and implications for flow paths. International Symposium on Japan-France KAIKO-TOKAI Project - Tectonics of Subduction in the Nankai Trough. Elsevier Science Bv, Tokyo, Japan, pp. 119-143.

Henry, P., Le Pichon, X., Lallemant, S., Lance, S., Martin, J.B., Foucher, J.P., FialaMedioni, A., Rostek, F., Guilhaumou, N., Pranal, V., Castrec, M., 1996. Fluid flow in and around a mud volcano field seaward of the Barbados accretionary wedge: Results from Manon cruise. Journal of Geophysical Research-Solid Earth 101 (B9), 20297-20323.

Hessler, R.R., Jumars, P.A., 1974. Abyssal community analysis from replicate box cores in the central North Pacific. Deep Sea Research 21, 185-209.

Hovland, M., Gardner, J.V., Judd, A.G., 2002. The significance of pockmarks to understanding fluid flow processes and geohazards. Geofluids 2 (2), 127-136.

Hubert-Ferrari, A., Barka, A., Jacques, E., Nalbant, S.S., Meyer, B., Armijo, R., Tapponnier, P., King, G.C.P., 2000. Seismic hazard in the Marmara Sea region following the 17 August 1999 Izmit earthquake. Nature 404 (6775), 269-273.

Hurlbert, S.H., 1971. The nonconcept of species diversity: a critique and alternative parameters. Ecology 52 (4), 577-586.

Iversen, N., Jørgensen, B.B., 1993. Diffusion coefficients of sulfate and methane in marine sediments: Influence of porosity. Geochimica et Cosmochimica Acta 57 (3), 571-578.

Jaccard, P., 1901. Dsitribution de la flore alpine dans le Bassin des Dranses et dans quelques régions voisines. Bulletin de la société vaudoise des sciences naturelles.

Jackson, D.A., 2005. PORTEST: a PROcustean randomization TEST of community environment concordance. Ecosciences 2, 297-303.

Jensen, P., Aagaard, I., Burke, R.A., Dando, P.R., Jorgensen, N.O., Kuijpers, A., Laier, T., Ohara, S.C.M., Schmaljohann, R., 1992. Bubbling Reefs In The Kattegat - submarine landscapes of carbonate-cemented rocks support a diverse ecosystem at methane seeps. Marine Ecology Progress Series 83 (2-3), 103-112.

Jerosch, K., Schluter, M., Pesch, R., 2006. Spatial analysis of marine categorical information using indicator kriging applied to georeferenced video mosaics of the deep-sea Hakon Mosby Mud volcano. Ecological Informatics 1 (4), 391-406.

Jost, G., 2007. Partitioning diversity into independant alpha and beta components. Ecology 88, 2427-2439.

Jost, L., 2006. Entropy and diversity. Oikos 113, 363-375.

Judd, A.G., Hovland, M., 2007. Seabed Fluid Flow - The Impact on Geology, Biology and the Marine Environment.

Jumars, P.A., Hessler, R.R., 1976. Hadal community structure - implications from Aleutian trench. Journal of Marine Research 34 (4), 547-560.

Kendall, M.G., 1938. A new measure of rank correlation. Biometrika 30 (1-2), 81-93.

Kindt, R., Coe, R., 2005. Tree diversity analysis. A manual and software for common statistical methods for ecological and biodiversity studies. World Agroforestry Centre (ICRAF). Nairobi.

Le Pichon, X., Foucher, J.P., Boulegue, J., Henry, P., Lallemant, S., Benedetti, M., Avedik, F., Mariotti, A., 1990. Mud Volcano Field Seaward Of The Barbados Accretionary Complex - A Submersible Survey. Journal of Geophysical Research-Solid Earth And Planets 95 (B6), 8931-8943.

Le Pichon, X., Sengor, A.M.C., Demirbag, E., Rangin, C., Imren, C., Armijo, R., Gorur, N., Cagatay, N., Mercier de Lepinay, B., Meyer, B., 2001. The active Main Marmara Fault. Earth and Planetary Science Letters 192 (4), 595.

Legendre, P., Gallagher, E.D., 2001. Ecologically meaningful transformations for ordination of species data. Oecologia 129 (2), 271-280.

Legendre, P., Legendre, L., 1998. Numerical ecology, 2nd English ed.

Levin, L.A., 2005. Ecology of cold seep sediments: interactions of fauna with flow, chemistry and microbes. Oceanography and Marine Biology - An Annual Review, Vol. 43. Crc Press-Taylor & Francis Group, Boca Raton, pp. 1-46.

Levin, L.A., Gage, J.D., 1998. Relationships between oxygen, organic matter and the diversity of bathyal macrofauna. Deep Sea Research Part II: Topical Studies in Oceanography 45 (1-3), 129.

Levin, L.A., Ziebis, W., Mendoza, G.F., Growney, V.A., Tryon, M.D., Mahn, C., Gieskes, J.M., Rathburn, A.E., 2003. Spatial heterogeneity of macrofauna at northern California methane seeps: influence of sulfide concentration and fluid flow. MEPS 265, 123-139.

Levin, L.A., Mendoza, G.F., 2007. Community structure and nutrition of deep methane-seep macrobenthos from the North Pacific (Aleutian) Margin and the Gulf of Mexico (Florida Escarpment). Marine Ecology-An Evolutionary Perspective 28 (1), 131-151.

Li, Y.-H., Gregory, S., 1974. Diffusion of ions in sea water and in deep-sea sediments. Geochimica et Cosmochimica Acta 38, 703-714.

Linke, P., Suess, E., Torres, M., Martens, V., Rugh, W.D., Ziebis, W., Kulm, L.D., 1994. In-Situ Measurement Of Fluid-Flow From Cold Seeps At Active Continental Margins. Deep-Sea Research Part I-Oceanographic Research Papers 41 (4), 721-739.

Liu, C., Whittaker, R.J., Ma, K., Malcolm, J.R., 2007. Unifying and distinguishing diversity ordering methods for comparing communities. Population Ecology 49, 89-100.

Luth, C., Luth, U., Gebruk, A.V., Thiel, H., 1999. Methane gas seeps along the oxic/anoxic gradient in the Black Sea: manifestations, biogenic sediment compounds and preliminary results on benthic ecology. Marine Ecology-Pubblicazioni Della Stazione Zoologica Di Napoli I 20 (3-4), 221-249.

Luth, U., Luth, C., 1998 Benthic meiofauna and macrofauna of a methane seep area south-west of the Crimean Peninsula, Black Sea. In: Luth U., Luth C., Thiel H. (Eds), MEGASEEPS- Methane Gas Seeps Exploration in the Black Sea. Berichte aus dem Zentrum fuer Meeres- und Klimatoforsch, Hamburg 14, 113-126.

Menot, L., Galéron, J., Olu, K., Caprais, J.C., Crassous, P., Khripounoff, A., Sibuet, M., 2009. Spatial heterogeneity of macrofaunal communities in and near a giant pockmark area in the deep Gulf of Guinea. Marine Ecology.

Milkov, A.V., 2000. Worldwide distribution of submarine mud volcanoes and associated gas hydrates. Marine Geology 167 (1-2), 29-42.

1094 Niemann, H., Duarte, J., Hensen, C., Omoregie, E., Magalhaes, V.H., Elvert, M.,
1095 Pinheiro, L.M., Kopf, A., Boetius, A., 2006a. Microbial methane turnover at mud
1096 volcanoes of the Gulf of Cadiz. Geochimica et Cosmochimica Acta 70 (21), 5336-
1097 5355.

1098 Niemann, H., Losekann, T., de Beer, D., Elvert, M., Nadalig, T., Knittel, K., Amann,
1099 R., Sauter, E.J., Schluter, M., Klages, M., Foucher, J.P., Boetius, A., 2006b. Novel
1100 microbial communities of the Haakon Mosby mud volcano and their role as a
1101 methane sink. Nature 443 (7113), 854-858.

1102 Oglesby, D.D., Mai, P.M., Atakan, K., Pucci, S., 2008. Dynamic models of
1103 earthquakes on the North Anatolian fault zone under the Sea of Marmara: Effect of
1104 hypocenter location. Geophysical Research Letters 35 (18), 4.

1105 Oksanen, J., Kindt, R., Legendre, P., O'Hara, B., Simpson, G.L., Solymos, P., Henry,
1106 M., Stevens, H., Wagner, H., 2008. Vegan: Community Ecology Package. R package
1107 version 1.15-1., pp. http://cran.r-project.org/, http://vegan.r-forge.r-project.org/.

1108 Olu, K., Lance, S., Sibuet, M., Henry, P., Fiala-Medioni, A., Dinet, A., 1997. Cold
1109 seep communities as indicators of fluid expulsion patterns through mud volcanoes
1110 seaward of the Barbados accretionary prism. Deep Sea Research Part I:
1111 Oceanographic Research Papers 44 (5), 811.

1112 Olu, K., Sibuet, M., Harmegnies, F., Foucher, J.P., Fiala-Médioni, A., 1996. Spatial
1113 distribution of diverse cold seep communities living on various diapiric structures of
1114 the southern Barbados prism. Progress in Oceanography 38 (4), 347-356.

1115 Olu-Le Roy, K., Caprais, J.C., Fifis, A., Fabri, M.C., Galeron, J., Budzinsky, H., Le
1116 Menach, K., Khripounoff, A., Ondreas, H., Sibuet, M., 2007. Cold-seep assemblages
1117 on a giant pockmark off West Africa: spatial patterns and environmental control.
1118 Marine Ecology-An Evolutionary Perspective 28 (1), 115-130.

1119 Olu-Le Roy, K., Sibuet, M., Fiala-Medioni, A., Gofas, S., Salas, C., Mariotti, A.,
1120 Foucher, J.-P., Woodside, J., 2004. Cold seep communities in the deep eastern
1121 Mediterranean Sea: composition, symbiosis and spatial distribution on mud
1122 volcanoes. Deep Sea Research Part I: Oceanographic Research Papers 51 (12),
1123 1915.

1124 Orphan, V.J., Ussler, W., Naehr, T.H., House, C.H., Hinrichs, K.U., Paull, C.K., 2004.
1125 Geological, geochemical, and microbiological heterogeneity of the seafloor around
1126 methane vents in the Eel River Basin, offshore California. Chemical Geology 205 (3-
1127 4), 265-289.

1128 Patil, G.P., Taillie, C., 1982. Diversity as a Concept and its Measurement. Journal of
1129 the American Statistical Association 77 (379), 548-561.

1130 Paull, C.K., Hecker, B., Commeau, R., Freeman-Lynde, R.P., Neumann, C., Corso,
1131 W.P., Golubic, S., Hook, J.E., Sikes, E., Curray, J., 1984. Biological communities at
1132 the Florida Escarpment resemble hydrothermal vent taxa. Science 226, 965-967.

1133 Pielou, E.C., 1969. An introduction to mathematical ecology, New York.

1134 Pierre, C., Fouquet, Y., 2007. Authigenic carbonates from methane seeps of the
1135 Congo deep-dea fan. Geo Mar Lett 27, 249-257.

1136 R, Development Core Team (2009). R: A Language and Environment for Statistical
1137 Computing. R Foundation for Statistical Computing. Vienna, Austria.

1138 Rathburn, A.E., Levin, L.A., Tryon, M., Gieskes, J.M., Martin, J.B., Pérez, M.E.,
1139 Fodrie, F.J., Neira, C., Fryer, G.J., Mendoza, G., McMillan, P.A., Kluesner, J.,
1140 Adamic, J., Ziebis, W., 2009. Geological and biological heterogeneity of the Aleutian
1141 margin (1965-4822 m). Progress in Oceanography 80 (1-2), 22-50.

1142 Ritt, B., Desbruyeres, D., Caprais, J.C., Khripounoff, A., Le Gall, C., Gauthier, O.,
1143 Buscail, R., Olu, K., Sarrazin, J., in preparation. Cold seep communities in the deep
1144 eastern Mediterranean Sea: composition, spatial patters and environmental control
1145 on the Mediterranean Ridge mud volcanoes.

1146 Robinson, C.A., Bernhard, J.M., Levin, L.A., Mendoza, G.F., Blanks, J.K., 2004.
1147 Surficial hydrocarbon seep infauna from the Blake Ridge (Atlantic Ocean, 2150 m)
1148 and the Gulf of Mexico (690-2240 m). Marine Ecology-Pubblicazioni Della Stazione
1149 Zoologica Di Napoli I 25 (4), 313-336.

1150 Sahling, H., Galkin, S.V., Salyuk, A., Greinert, J., Foerstel, H., Piepenburg, D.,
1151 Suess, E., 2003. Depth-related structure and ecological significance of cold-seep
1152 communities-a case study from the Sea of Okhotsk. Deep Sea Research Part I:
1153 Oceanographic Research Papers 50 (12), 1391.

1154 Sahling, H., Rickert, D., Lee, R.W., Linke, P., Suess, E., 2002. Macrofaunal
1155 community structure and sulfide flux at gas hydrate deposits from the Cascadia
1156 convergent margin, NE Pacific. Marine Ecology Progress Series 231, 121-138.

1157 Salas, C., Woodside, J., 2002. Lucinoma kazani n. sp. (Mollusca: Bivalvia): evidence
1158 of a living benthic community associated with a cold seep in the Eastern
1159 Mediterranean Sea. Deep Sea Research Part I: Oceanographic Research Papers 49
1160 (6), 991-1005.

1161 Sarradin, P.M., Caprais, J.C., 1996. Analysis of dissolved gases by headspace
1162 sampling gas chromatography with column and detector switching. Preliminary
1163 results. Analytical Communications 33 (10), 371-373.

1164 Sarrazin, J., Juniper, S.K., 1999. Biological characteristics of a hydrothermal edifice
1165 mosaic community. Marine Ecology-Progress Series 185, 1-19.

1166 Sengor, A.M.C., Tuysuz, O., Imren, C., Sakinc, M., Eyidogan, H., Gorur, G., Le
1167 Pichon, X., Rangin, C., 2005. The North Anatolian Fault: a new look. Annual Review
1168 Of Earth and Planetary Sciences 33, 37-112.

1169 Sergeeva, N.G. and Gulin, M.B., 2007. Meiobenthos from an active methane
1170 seepage area in the NW Black Sea. Marine Ecology 28: 152-159.

1171 Shannon, C.E., 1948. A mathematical therory of communication. Bell System
1172 Technical Journal 27, 379-423, 623-656.

1173 Sibuet, M., Olu, K., 1998. Biogeography, biodiversity and fluid dependence of deep-
1174 sea cold-seep communities at active and passive margins. Deep Sea Research Part
1175 II: Topical Studies in Oceanography 45 (1-3), 517.

1176 Simpson, E.H., 1949. Measurement of Diversity. Nature 163, 688.

1177 Sommer, S., Linke, P., Pfannkuche, O., Schneider, R., Reitz, A., Haeckel, M., Flögel,
1178 S., Hensen, C., 2009. Seabed methane emissions and the habitat of frenulate
1179 tubeworms on the Captain Arutyunov mud volcano (Gulf of Cadiz). Marine Ecology
1180 Progress Series 382, 69-86.

1181 Sommer, S., Linke, P., Pfannkuche, O., Niemann, H., Treude, T., 2009b. Benthic
1182 respiration in a seep habitat dominated by dense beds of ampharetid polychaetes at
1183 the Hikurangi Maring (new Zealand). Marine Geology doi:
1184 10.1016/j.margo.2009.06.003.

1185 Sturany, R., 1896. Zoologische Ergebnisse VII. Mollusken I (Prosobranchier und
1186 Opisthobranchier; Scaphopoden; Lamellibranchier) gesammelt von S.M. Schiff "Pola"
1187 1890-18. Denkschriften der Kaiserlichen Akademie der Wissenschaften,
1188 Mathematische-Naturwissenschaftlischen Classe 63, 1-36, pl.31-32.

1189 Teichert, B.M.A., Bohrmann, G., Suess, E., 2005. Chemoherms on Hydrate Ridge -
1190 Unique microbially-mediated carbonate build-ups growing into the water column.
1191 Palaeogeography Palaeoclimatology Palaeoecology 227 (1-3), 67-85.

1192 Thistle, D., 2003. The Deep-Sea Floor: An Overview. Ecosystems of The Deep
1193 Ocean. Elsevier Science Bv, pp. 5-37.

1194 Toki, T., Tsunogai, U., Gamo, T., Kuramoto, S., Ashi, J., 2004. Detection of low-
1195 chloride fluids beneath a cold seep field on the Nankai accretionary wedge off
1196 Kumano, south of Japan. Earth and Planetary Science Letters 228 (1-2), 37-47.

1197 Tothmérész, B., 1998. On the characterization of scale-dependant diversity.
1198 Abstracta Bonatica 22, 149-156.

1199 Torres, M.E., McManus, J., Hammond, D.E., de Angelis, M.A., Heeschen, K.U.,
1200 Colbert, S.L., Tryon, M.D., Brown, K.M., Suess, E., 2002. Fluid and chemical fluxes
1201 in and out of sediments hosting methane hydrate deposits on Hydrate Ridge, OR, I:
1202 hydrological provinces. Earth and Planetary Science Letters 201 (3-4), 525-540.

1203 Tunnicliffe, V., Juniper, S.K., Sibuet, M., 2003. Reducing environments of the Deep-
1204 Sea Floor. Ecosystems of the Deep Ocean. Elsevier Science Bv, Amsterdam, pp. 81-
1205 110.

1206 Van Aartsen, J.J., Borghi, C., Giusti, F., 1989. Remarks on the genus Benthonella
1207 (Rissoidae) in Europe. La Conchiglia.

1208 Van Dover, C.L., Aharon, P., Bernhard, J.M., Caylor, E., Doerries, M., Flickinger, W.,
1209 Gilhooly, W., Goffredi, S.K., Knick, K.E., Macko, S.A., Rapoport, S., Raulfs, E.C.,
1210 Ruppel, C., Salerno, J.L., Seitz, R.D., Sen Gupta, B.K., Shank, T., Turnipseed, M.,
1211 Vrijenhoek, R., 2003. Blake Ridge methane seeps: characterization of a soft-

sediment, chemo synthetically based ecosystem. Deep-Sea Research Part I-Oceanographic Research Papers 50 (2), 281-300.

Van Gaever, S., Moodley, L., de Beer, D., Vanreusel, A., 2006. Meiobenthos at the Arctic Hakon Mosby Mud Volcano, with a parental-caring nematode thriving in sulphide-rich sediments. Marine Ecology Progress Series 321, 143-155.

Vanreusel, A., Andersen, A.C., Boetius, A., Connelly, D., Cunha, M.R., Decker, C., Hilario, A., Kormas, K.A., Maignien, L., Olu, K., Pachiadaki, M., Ritt, B., Rodrigues, C., Sarrazin, J., Tyler, P., Van Gaever, S., Vanneste, H., 2009. Biodiversity of Cold Seep Ecosystems Along the European Margins. Oceanography 22 (1), 110-127.

Wallmann, K., Linke, P., Suess, E., Bohrmann, G., Sahling, H., Schluter, M., Dahlmann, A., Lammers, S., Greinert, J., von Mirbach, N., 1997. Quantifying fluid flow, solute mixing, and biogeochemical turnover at cold vents of the eastern Aleutian subduction zone. Geochimica et Cosmochimica Acta 61 (24), 5209-5219.

Ziebis, W., Forster, S., Huettel, M., Jorgensen, B.B., 1996. Complex burrows of the mud shrimp *Callianassa truncata* and their geochemical impact in the sea bed. Nature 382, 619-622.

Zitter, T.A.C., Henry, P., Aloisi, G., Delaygue, G., Cagatay, M.N., de Lepinay, B.M., Al-Samir, M., Fornacciari, F., Tesmer, M., Pekdeger, A., Wallmann, K., Lericolais, G., 2008. Cold seeps along the main Marmara Fault in the Sea of Marmara (Turkey). Deep-Sea Research Part I-Oceanographic Research Papers 55 (4), 552-570.

1240

Table 1

Sample locations, depth, sampling effort, and gear used to perform physico-chemical and faunal sampling in the three most common microhabitats of the north-eastern Central basin in the Marmara Sea explored during the MarNaut cruise in 2007. The length of the sediment cores and the estimated surface area of each carbonate crust sample are also reported.

Microhabitat types	**Latitude (°N)**	**Longitude (°E)**	**Depth (m)**	**Physico-chemical sampling**		**Faunal sampling**
				Interface water	Pore water in sediments	
Bioturbated sediments (Bio)	40°51.28’	28°10.20’	1122	1x1 minute MicroCat measurements: temperature, salinity	2 tube cores: SO_4^{2-} , Cl^- profiles	1 blade core: Bio (13 cm)
Reduced sediments (Red)	40°51.27’	28°10.19’	1121	3x1 minute MicroCat measurements: temperature, salinity 3x2 water samples: CH_4, pH	3x2 tube cores: O_2, SO_4^{2-} , Cl^- profiles	3 blade cores: Red1 (12 cm) Red2 (20 cm) Red3 (12 cm)
Carbonate crusts (CC)	40°51.27’	28°10.19’	1111	None	None	3 pieces of crust: CC1 (459 cm²) CC2 (368 cm²) CC3 (189 cm²) + CC_{Box}

1241
1242
1243

Table 2
Visual observations of sediment colour in the Bio and Red microhabitats. Temperature, salinity, dissolved oxygen and methane concentrations and pH measurements at the sediment-water interface in microhabitat samples from the Marmara Sea are also given (MarNaut cruise, 2007).

	Visual observations	Temperature	Salinity	$[O_2]$	$[CH_4]$	pH
Bio	Brown sediments at the top, reduced sediments the bottom	14.52	38.77	-	-	-
Red1	Reduced sediments throughout core	14.52	38.76	22.9 ± 13.1 µM	0.33 ± 0.04 µM	7.93 ± 0.01
Red2		14.52	38.76	22.8 µM	0.7 ± 0.28 µM	7.94 ± 0.02
Red3		14.52	38.77	50.9 ± 0.3 µM	0.14 ± 0.03 µM	7.89 ± 0.04

Table 3
Relative macrofaunal (>250 µm) abundances (%) and total absolute abundances in the three microhabitats studied: bioturbated sediment (Bio, n=1), reduced sediment (Red, n=3) and carbonate crust (CC, n=3) microhabitats. Specimens recovered at the bottom of the sampling box (CC_{Box}) are also reported. Total relative abundance from each taxonomic group is highlighted in bold. All samples are from the north-eastern Central basin in the Marmara Sea (MarNaut cruise, 2007). * Taxonomic level used for alpha-diversity analyses.

Taxonomic groups		**Reduced sediments**				**Carbonate crusts**				
	Bio	**Red1**	**Red2**	**Red3**	**Avg. ± SD**	**CC1**	**CC2**	**CC3**	**Avg.±SD**	**CC_{Box}**
Porifera (Total)	**0**	**0**	**0**	**0**	**0**	**0**	**0**	**0**	**0**	**0.65**
Demospongia*	0	0	0	0	0	0	0	0	0	0.65
Cnidaria (Total)	**0**	**0**	**0**	**0**	**0**	**8.24**	**1.16**	**1.08**	**3.49±4.11**	**0**
Anthozoa - Zoantharia										
Parazoanthidae*	0	0	0	0	0	7.62	0.12	0	2.58±4.37	0
Isozoanthus sp.1	*0*	*0*	*0*	*0*	*0*	*0.12*	*0.12*	*0*	*0.08±0.07*	*0*
Isozoanthus sp.2	*0*	*0*	*0*	*0*	*0*	*7.50*	*0*	*0*	*2.50±4.33*	
Anthozoa - Actiniaria										
Sagartiidae*	0	0	0	0	0	0.62	1.04	1.08	0.84±0.23	0
Sagartiogeton sp.	*0*	*0*	*0*	*0*	*0*	*0.62*	*0.81*	*1.08*	*0.84±0.23*	*0*
Medusozoa – Scyphozoa*	0	0	0	0	0	0	0.23	0	0.08±0.13	0
Polychaeta (Total)	**36.02**	**99.23**	**98.25**	**90.90**	**96.13±4.54**	**16.60**	**17.58**	**3.23**	**12.47±8.02**	**32.03**
Ampharetidae*	0.54	29.46	3.52	54.54	29.17±25.52	4.31	7.45	2.15	4.64±2.67	11.77
Capitellidae*	0	0	0	0	0	0	0.12	0	0.04±0.07	0
Cirratulidae*	0	0	0	0	0	4.55	0.35	0	1.63±2.53	1.96
Cossuridae*	1.61	0	0	0	0	0	0	0	0	0
Dorvilleidae*	0	69.77	91.23	27.27	62.76±32.55	5.04	6.17	1.08	4.10±2.68	2.61
Flabelligeridae*	1.08	0	0	0	0	0	0	0	0	0
Hesionidae*	0	0	0	0	0	1.72	1.40	0	1.04±0.91	1.96
Lumbrineridae*	2.69	0	0	0	0	0	0	0	0	0
Paraonidae*	20.43	0	0	0	0	0	0	0	0	0
Pholoidae*	0	0	1.75	0	0.58±1.01	0	0	0	0	0
Phyllodocidae*	0.54	0	0	0	0	0	0	0	0	0.66
Spionidae*	5.90	0	0	0	0	0.98	2.09	0	1.03±1.05	13.07
Syllidae*	3.23	0	0	0	0	0	0	0	0	0
Unid. Families*	0	0	1.75	9.09	3.62±4.82	0	0	0	0	0
Bivalvia (Total)	**50.01**	**0.77**	**0**	**0**	**0.26±0.45**	**10.33**	**8.96**	**68.81**	**29.37±34.17**	**24.84**
Lucinidae*	19.89	0	0	0	0	0	0	0	0	1.31
Lucinoma kazani	*1.61*	*0*	*0*	*0*	*0*	*0*	*0*	*0*	*0*	*0*
Myrtea amorpha	*0*	*0*	*0*	*0*	*0*	*0*	*0*	*0*	*0*	*1.31*
Unid. Lucinidae	*18.28*	*0*	*0*	*0*	*0*	*0*	*0*	*0*	*0*	*0*
Mytilidae*	0	0	0	0	0	10.08	8.84	68.81	29.25±34.27	9.15
Mytilidae nov. sp.	*0*	*0*	*0*	*0*	*0*	*10.08*	*8.84*	*68.81*	*29.25±34.27*	*9.15*
Vesicomyidae*	2.15	0	0	0	0	0	0	0	0	7.84
Isorropodon perplexum	*1.61*	*0*	*0*	*0*	*0*	*0*	*0*	*0*	*0*	*7.84*
Unid. Vesicomyidae	*0.54*	*0*	*0*	*0*	*0*	*0*	*0*	*0*	*0*	*0*
Yoldiidae*	5.38	0.77	0	0	0.26±0.45	0	0	0	0	0
Yoldiella striolata	*5.38*	*0.77*	*0*	*0*	*0.26±0.45*	*0*	*0*	*0*	*0*	*0*
Sareptidae*	2.69	0	0	0	0	0	0	0	0	0
Montacutidae*	16.67	0	0	0	0	0	0	0	0	0
Unid. Famillies*	3.23	0	0	0	0	0.25	0.12	0	0.12±0.12	6.54

Gastropoda (Total)	**1.61**	**0**	**1.75**	**9.10**	**3.62 ± 4.82**	**64.58**	**72.18**	**26.88**	**54.54±24.26**	**40.52**
Pyramidellidae*	0.54	0	0	0	0	0	0	0	0	0
Odostomia sp.	*0.54*	*0*	*0*	*0*	*0*	*0*	*0*	*0*	*0*	*0*
Trochidae*	0	0	0	0	0	0	0	1.08	0.36±0.62	0
Putseysia wiseri	*0*	*0*	*0*	*0*	*0*	*0*	*0*	*1.08*	*0.36±0.62*	*0*
Elachisinidae*	0	0	0	0	0	64.58	72.18	25.80	54.18±24.87	40.52
Laeviphitus verduini	*0*	*0*	*0*	*0*	*0*	*64.58*	*72.18*	*25.80*	*54.18±24.87*	*40.52*
Xyladisculidae*	0	0	0	4.55	1.52±2.62	0	0	0	0	0
Xylodiscula sp.	*0*	*0*	*0*	*4.55*	*1.52±2.62*	*0*	*0*	*0*	*0*	*0*
Unid. Families*	1.07	0	1.75	4.55	2.10±2.29	0	0	0	0	0
Aplacophora (Total)	**2.14**	**0**	**0**	**0**	**0**	**0**	**0**	**0**	**0**	**0**
Chaetodermatidae*	2.14	0	0	0	0	0	0	0	0	0
Falcidens gutturosus	*1.61*	*0*	*0*	*0*	*0*	*0*	*0*	*0*	*0*	*0*
Prochaetoderma sp.	*0.53*	*0*	*0*	*0*	*0*	*0*	*0*	*0*	*0*	*0*
Crustacea (Total)	**5.38**	**0**	**0**	**0**	**0**	**0.25**	**0.12**	**0**	**0.12±0.12**	**1.96**
Amphipoda-Gammarida										
Oedicerotidae*	3.76	0	0	0	0	0	0	0	0	0
Perioculodes aff. *longimanus*	*3.76*	*0*	*0*	*0*	*0*	*0*	*0*	*0*	*0*	*0*
Lysianassidae*	0	0	0	0	0	0.25	0.12	0	0.12±0.12	1.96
Lysianassa longicornis	*0*	*0*	*0*	*0*	*0*	*0.25*	*0.12*	*0*	*0.12±0.12*	*1.96*
Cumacea										
Diastylidae*	0.54	0	0	0	0	0	0	0	0	0
Diastyloides serrata	*0.54*	*0*	*0*	*0*	*0*	*0*	*0*	*0*	*0*	*0*
Unid. Famillies (juvenile)*	1.08	0	0	0	0	0	0	0	0	0
Echinodermata (Total)	**2.15**	**0**	**0**	**0**	**0**	**0**	**0**	**0**	**0**	**0**
Echinoida-Spatangoida										
Brissidae*	2.15	0	0	0	0	0	0	0	0	0
Brissopsis sp.	*2.15*	*0*	*0*	*0*	*0*	*0*	*0*	*0*	*0*	*0*
Total abundances (number of individuals)	**186**	**129**	**57**	**22**	**69±55**	**813**	**859**	**93**	**588±430**	**153**

Table 4
Relative meiofaunal abundances (%) and total absolute abundances in the three microhabitats studied: bioturbated sediment (Bio, n=1), reduced sediment (Red, n=3) and carbonate crust (CC, n=3) microhabitats. All samples are from the north-eastern part of the Central basin of the Marmara Sea (MarNaut cruise, 2007). (**) This proportion is largely underestimated since only the meiofauna >250 µm was sampled. No meiofauna was found in CC_{Box}. * Taxonomic level used for alpha-diversity analyses.

Taxa		**Reduced sediments**				**Carbonate crusts**			
	Bio	**Red1**	**Red2**	**Red3**	**Avg.±SD**	**CC1**	**CC2**	**CC3**	**Avg.±SD**
Nematoda* (Total)	**79.88**	**99.81**	**99.74**	**100**	**99.85±0.13**	**79.03**	**95.68**	**85.00**	**86.58±8.43**
Crustacea (Total)	**18.66**	**0.19**	**0.26**	**0**	**0.15±0.13**	**20.97**	**4.32**	**15.00**	**13.43±8.44**
Copepoda-Harpacticoida									
Miraciidae*									
Typhamphiascus confusus	13.12	0	0	0	0	16.83	0.32	15.00	10.72±9.05
Typhamphaiscus sp.	0.29	0	0	0	0	0	0	0	0
Ameiridae*									
Amphiascus sp.	*0*	*0*	*0*	*0*	*0*	*1.65*	*1.28*	*0*	*0.98±0.87*
Ameira longipes	*0*	*0*	*0*	*0*	*0*	*0.33*	*0*	*0*	*0.11±0.19*
Ameridae n. gen.	*0*	*0*	*0*	*0*	*0*	*0.17*	*1.12*	*0*	*0.43±0.60*
Haifamera archibenthoica	*1.46*	*0*	*0*	*0*	*0*	*0*	*0.16*	*0*	*0.05±0.09*
Pseudotachidiidae*									
Pseudotachidius coronatus	*0.29*	*0*	*0*	*0*	*0*	*0*	*0*	*0*	*0*
Tisbidae*									
Tisbella sp.	*0*	*0*	*0*	*0*	*0*	*0.83*	*0.64*	*0*	*0.49±0.43*
Laophontidae*									
Archesola typhlops	0	0	0	0	0	0.17	0	0	0.06±0.10
Harpacticoida Juvenile	1.75	0	0	0	0	0.99	0.64	0	0.54±0.50
Copepoda-Cyclopoida									
Cyclopinidae*									
Cyclopina sp.1	0.88	0.15	0	0	0.05±0.09	0	0	0	0
Cyclopina sp.2	0.29	0	0	0	0	0	0	0	0
Copepoda-Calanoida									
Unid. Calanoida*	0	0	0	0	0	0	0.16	0	0.05±0.09
Ostracoda									
Cytherellidae*									
Cytherella vulgata	*0.29*	*0*	*0*	*0*	*0*	*0*	*0*	*0*	*0*
Potocyrpididae*									
Proponcypris cf. levis	*0.29*	*0.04*	*0*	*0*	*0.01±0.02*	*0*	*0*	*0*	*0*
Proponcypris sp.1	*0*	*0*	*0.13*	*0*	*0.04±0.07*	*0*	*0*	*0*	*0*
Proponcypris sp.2	*0*	*0*	*0.13*	*0*	*0.04±0.07*	*0*	*0*	*0*	*0*
Chelicerata (Total)	**1.46**	**0**	**0**	**0**	**0**	**0**	**0**	**0**	**0**
Unid. familly Acarina*	1.46	0	0	0	0	0	0	0	0
% meiofauna / Total fauna**	64.8	95.4	93.3	98.3	95.7±2.5	42.7	42.2	17.7	34.2±14.3
Total abundances (number of individuals)	343	2 696	797	1 274	1 589±988	606	626	20	417±344

1281

1282

Table 5
Biological descriptors of the three sampled microhabitats in the Marmara Sea. The numbers equivalents of Shannon and Simpson indices are given in italics. The highest values are highlighted in bold. Meiofaunal data is presented notwithstanding the incomplete sampling protocol.

Biological descriptors	Bioturbated sediments	Reduced sediments	Carbonate crusts
Macrofauna -dominant	Bivalves and polychaetes, reaching respectively 50 and 36% of total abundance	Large dominance of polychaetes, reaching a mean of 96.1% of total abundance (Dorvilleidae, Ampharetidae)	Gastropods and bivalves in various proportions, reaching a mean of 54.5 and 29.4% of total abundance, respectively
Macrofauna -others	Gastropods, crustaceans, aplacophora, chelicerates, echinoids	Bivalves, gastropods	Cnidarians, polychaetes, crustaceans
Macrofaunal densities	9 300 ind/m^2	3 433 ± 2 740 ind/m^2	**15 325 ± 9 440 ind/m^2**
Jaccard's similarity coefficient[a]	-	0.44	0.54
Symbiont-bearing fauna	3.8%	0%	**8.9 – 68.8%**
Mean total biomass (kg ww/m^2)	0.0018	0.0019 ± 0.001	**0.806 ±0. 25**
Macrofaunal diversity indices			
Richness (S)[b]	**21**	7	18
Shannon (H_e')[b] *Exp (H_e')*	**2.42** *11.25*	0.77 *2.16*	1.37 *3.94*
Simpson (D_{GS})[b] *($1/1-D_{GS}$)*	**0.87** ***7.73***	0.43 *1.76*	0.56 *2.29*
Evenness (J')[b]	**0.79**	0.39	0.47
Meiofauna -dominant	Nematodes with 81% of the total abundance	Nematodes with nearly 99.9% of the total abundance	Nematodes with 86.6% of the total abundance
Meiofauna -others	Copepods, nauplii, ostracods (19%)	Copepods, ostracods (0.1%)	Copepods (13.4%)
Meiofaunal densities	16 900 ind/m^2	**79 450 ± 49 396 ind/m^2**	10 424 ± 8 331 ind/m^2
Jaccard's similarity coefficient[a]	-	0.50	0.52
Meiofaunal diversity indices			
Total richness (S)[b]	**9**	3	6
Copepoda richness (S)[b]	**5**	1	5
Ostracoda richness (S)[b]	**2**	1	0
Acarina richness (S)[b]	**1**	0	0
Shannon (H_e')[b] *Exp (H_e')*	**0.76** *2.14*	0.01 *1.01*	0.47 *1.60*
Simpson (D_{GS})[b] *($1/1-D_{GS}$)*	**0.35** ***1.53***	0.002 *1.00*	0.22 *1.28*
Evenness (J')[b]	**0.34**	0.01	0.26

1283

[a] Mean Jaccard's similarity coefficient computed without CC_{Box},
[b] Diversity indices are given for macrofaunal and meiofaunal data with CC_{Box} included in both case.

Table 6
Review of the characteristics of different cold seep sites described by different authors, in terms of habitat, dominant fauna and related environmental conditions. This non-exhaustive list was compiled according to the availability of environmental data. SS: soft sediments, Co: concretions, Co/SS: concretions surrounded by soft sediments, GH/SS: gas hydrates within soft sediments.

Sites	Habitat type	Substratum	Dominant fauna	O_2 µmol/l	CH_4 µmol/l	SO_4^{2-} mmol/l	Authors
Gulf of Cadiz Cap. Arutyunov MV	Siboglinidae fields	SS	*Siboglinum poseidoni*	No data	0.3 – 1.1	30	Niemann et al., 2006a; Sommer et al., 2009a
Hydrate Ridge Southern Summit	Clam beds	SS	*Calyptogena pacifica, C. kilmeri*	20	0.6	28	Sahling et al., 2002; Torres et al., 2002
	Microbial mats	GH/SS	*Beggiatoa sp.*	20	1	28	"
Olimpi field - MedRidge Napoli MV	Siboglinidae bushes	SS	*Lamellibrachia* aff. *anaximandri*	202 – 212	0.35	31	Ritt et al., in prep.
	Carbonate crusts	Co	*Lurifax vitreus,* Porifera	196 – 199	2.27 – 4.29	31	"
Anaximandre Mounds Amsterdam MV	Reduced sediments	SS	*Isorropodon* aff. *perplexum*	188 - 192	12.5	28 - 31	"
	Carbonate crusts	Co	Serpulid polychaetes	194 – 202	0.25 – 0.6	31	"
Nile deep-sea fan Cheops MV	Reduced sediments	SS	Spionid, hesionid polychaetes	No data	3.7 – 7.7	No data	"
Eel River Basin	Clam beds	SS	*Calyptogena pacifica*	25-100	1 000	6.5	Levin et al., 2003; Orphan et al., 2004
	Microbial mats	GH/SS	*Beggiatoa sp.*	< 0.1	6500	6.3	"
Gulf of Mexico Green Canyon	Mussel beds	SS	*Bathymodiolus childressi*	129	21	30	Aharon et Fu, 2003; Bergquist et al., 2005
Alaska margin off Unimak island	Clam beds	SS	*Vesicomya extenta, V. diagonalis*	200	No data	28	Rathburn et al., 2009
	Siboglinidae fields	SS	*Siphonobrachia sp.*	140	No data	28	"
New Zealand margin	Ampharetidae fields	SS	Ampharetid polychaetes	197	1962	No data	Sommer et al., 2009b
Gulf of Guinea Giant pockmark Regab	Calyptogena beds	SS	*Calyptogena regab, Vesicomya* aff. *chuni*	211 – 238	0.4 – 3.4	No data	Olu-Le Roy et al., 2007
	Mytilidae Beds	SS/Co	*Bathymodiolus* aff. *boomerang*	230 – 240	0.7 – 23.2	No data	"

	Siboglinidae fields	Co	*Escarpia southwardae*	218 – 232	0.63 – 2.43	No data	"
Norwegian margin Håkon Mosby MV	Siboglinidae fields	SS	*Oligobrachia haakonmosbiensis, Siboglinum contortum*	270	0.7	28	Niemann et al., 2006b
	Microbial mats	SS	*Beggiatoa sp.*	270	0.3	28	"
	Centre	SS	Meiofauna (Copepoda)	270	5.7	28	Niemann et al., 2006b; Van Gaever et al., 2006
Nankaï Trench Off Kumano	Clams beds	SS	*Calyptogena* spp.	No data	0.006	28.3	Toki et al., 2004
	Tubeworms	SS	Vestimentiferan?	No Data	0.006 – 300	28.2	"
	Microbial mats	SS		No Data	0.2 – 300	28.5	"
This study	Reduced sediments	SS	Ampharetid, dorvilleid polychaetes	18 – 51	0.14 – 0.7	19 – 26	Ritt et al.
	Bioturbated sediments	SS	Paraonid polychaetes, lucinid bivalves	No data	No data	31	"
	Carbonate crusts	Co	*Idas sp. nov.*	No data	No data	No data	"

Resume of the range of chemical concentrations for the different substratum and assemblage types (all studies combined). Higher values are highlighted in bold.

Substratum	**Dominant fauna**	**O_2 µmol/l**	**CH_4 µmol/l**	**SO_4^{2-} mmol/l**
GH/SS	Microbial mats	< 0.1 - 20	1 **– 6 500**	6.3 - 28
SS	Polychaetes	18 - **270**	0.14 - 1962 (0.006)	19 - **31**
	Bivalves	20 - 238	0.4 - 1000 (0.006)	6.5 - **31**
	Microbial mats	**270**	0.2 - 300	28 - 28.5
	Copepods	**270**	5.7	28
SS/Co	Bivalves	230 - 240	0.7 - 23.2	
Co	Gastropods		2.27 - 4.29	
	Polychaetes	194 - 232	0.25 - 2.43	31

1290
1291